Published in final edited form as:
Chem Res Toxicol. 2023 March 20; 36(3): 402–419. doi:10.1021/acs.chemrestox.2c00344.

Evaluation of Per- and Poly fluoroalkyl Substances (PFAS) *in vitro* toxicity testing for developmental neurotoxicity

Kelly E. Carstens[†], **Theresa Freudenrich**[†], **Kathleen Wallace**[†], **Seline Choo**[‡], **Amy Carpenter**[‡], **Marci Smeltz**[§], **Matthew S. Clifton**[§], **W. Matthew Henderson**[§], **Ann M. Richard**[†], **Grace Patlewicz**[†], **Barbara A. Wetmore**[†], **Katie Paul Friedman**[†], **Timothy Shafer**[†]

[†]Center for Computational Toxicology and Exposure, ORD, US EPA, RTP, NC 27711

[‡]Oak Ridge Institute for Science and Education (ORISE), Oak Ridge, TN 37830

[§]Center for Environmental Measurement and Modeling, ORD, US EPA, RTP, NC 27711

Abstract

Per- and poly fluoroalkyl substances (PFAS) are a diverse set of commercial chemicals widely detected in humans and the environment. However, only a limited number of PFAS are associated with epidemiological or experimental data for hazard identification. To provide developmental neurotoxicity (DNT) hazard information, the work herein employed DNT new approach methods (NAMs) to generate *in vitro* screening data for a set of 160 PFAS. The DNT NAMs battery was comprised of the microelectrode array neuronal network formation assay (NFA) and high-content imaging (HCI) assays to evaluate proliferation, apoptosis, and neurite outgrowth. The majority of PFAS (118/160) were inactive or equivocal in the DNT NAMs, leaving 42 active PFAS that decreased measures of neural network connectivity and neurite length. Analytical quality control indicated 43/118 inactive PFAS samples and 10/42 active PFAS samples were degraded; as such, careful interpretation is required as some negatives may have been due to loss of the parent PFAS, and some actives may have resulted from a mixture of parent and/or degradants of PFAS. PFAS containing a perfluorinated carbon (C) chain length ≥8, a high C:fluorine ratio, or a carboxylic acid moiety were more likely to be bioactive in the DNT NAMs. Of the PFAS positives in DNT NAMs, 85% were also active in other EPA ToxCast assays, whereas 79% of PFAS inactives in the DNT NAMs were active in other assays. These data demonstrate that a subset of PFAS perturb neurodevelopmental processes *in vitro* and suggest focusing future studies of DNT on PFAS with certain structural feature descriptors.

Graphical Abstract

Corresponding author: Kelly E Carstens, 109 T.W. Alexander Drive, Mail Drop D130-A, Research Triangle Park, NC 27711, Carstens.kelly@epa.gov, Tel. 919-541-3834.

Supporting Information

- Supporting Information PDF includes Figures S1-11 and Supporting Information Methods as mentioned in the text.
- Supporting Information Tables includes tables S1-11 as mentioned in the text.

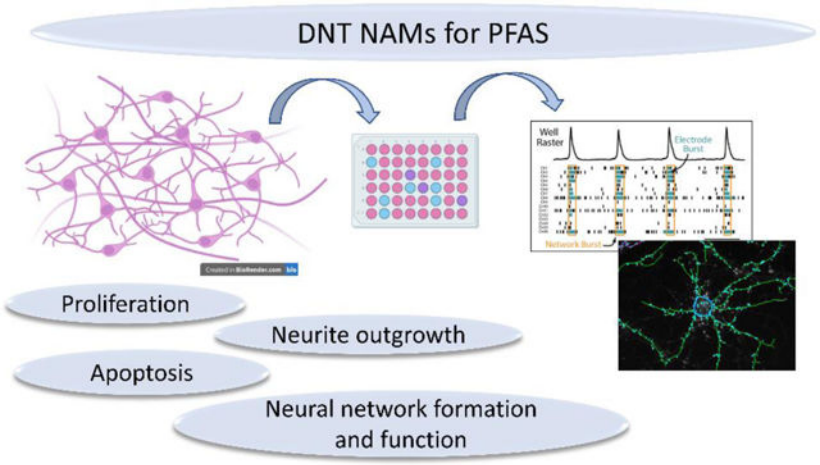

Introduction

Per- and poly fluoroalkyl substances (PFAS) are structurally diverse synthetic chemicals that are detected in the environment and in humans. PFAS have widespread commercial and industrial applications, such as water- and oil- repellents, surfactants, surface protectors, and fire-fighting foams. As of 2021, the OECD adopted a broad definition of PFAS that requires a minimum of one perfluorinated carbon, which results in a list of PFAS that may approach 40,000 substances, with more stringent definitions of PFAS structures resulting in shorter lists in the thousands[1–2]. Only a small number of legacy PFAS have been extensively evaluated for adverse human health potential, such as perfluorooctanoic acid (PFOA) and perfluorooctane sulfonic acid (PFOS), which are currently under regulation internationally[3–5]. Given widespread human exposure to PFAS, and the limited empirical information available for many PFAS[6], further predicting and characterizing hazard(s) associated with PFAS is a global interest.

Per- or poly- fluorinated carbon chains bonded to different functional groups such as carboxylic acid or sulfonic acid groups constitute the core structure of PFAS[1, 7]. The length of the fluorinated carbon chain results in varying physicochemical properties that influence their thermal stability and bioaccumulation. Long-chain PFAS have been identified as highly persistent, bioaccumulative, and toxic (OECD, 2013) and have been detected in the environment[8], biota[9] and in humans[10]. Examples of long-chain PFAS include perfluorocarboxylic acids with greater than 8 carbons in the chain, such as PFOA, or perfluoroalkane sulfonic acids (PFSAs) with greater than 6 carbons in the chain, such as perfluorohexane sulfonic acid (PFHxS) and PFOS. The study of PFAS absorption, accumulation, and distribution in the human brain is currently limited; however, PFAS have been detected in the brain of humans and wildlife species[11–13] In marine mammals, the abundance of PFAS in the brain was found to increase with carbon chain length of ≥10, demonstrating a correlation between the carbon chain length and the concentration of PFAS in the brain and also suggesting that PFAS with short chain length may cross the blood-brain barrier less efficiently[14].

Little is known about the effects of PFAS exposure on the developing human nervous system. However, PFAS such as, PFOA, PFOS, PFHxS, and perfluorononanoic acid (PFNA), are known to cross the placental barrier, and PFOA has been associated with fetal growth restrictions[15–17]. Recent systematic reviews of available human epidemiological studies found that associations between perinatal PFAS exposure and adverse neurodevelopmental outcome are inconsistent and inconclusive[18–19]. For example, one study found prenatal exposure to PFOA, but not PFOS, was associated with lower mental development in girls at 6 months of age but not at 18 months of age[20]. Another study found prenatal exposure to PFOS, but not PFOA, was associated with gross motor development deficits at two years of age[21]. Increased risk of attention deficit/hyperactivity disorder and autism spectrum disorders have been associated with perinatal exposures to PFAS including PFOS, PFOA, PFNA, and PFHxS, but findings are inconsistent between studies[22–28]. Finally, numerous studies report no association of perinatal PFOS and PFOA exposure with cognitive development at various postnatal ages[29–31]. There is some evidence of neurodevelopmental impairments in experimental animal models exposed to PFOS and PFOA[32–35], however limitations of using animal studies to predict human effects, coupled with the inconsistent findings from human epidemiology studies, precludes definitive conclusions regarding the effects of PFAS on neurological outcomes. Further, human and animal model data are lacking for most PFAS.

To address these limitations, the work herein employed DNT new approach methodologies (NAMs) to generate high-throughput *in vitro* toxicity data for PFAS[36–37]. Given that no single *in vitro* screening assay can recapitulate all critical processes of neurodevelopment due to temporal and biological complexity[38], the integration of *in vitro* assays representing diverse neurological processes across development is critical for understanding the DNT potential of PFAS. A set of 160 PFAS, constituting the Tier 1 testing portion of EPA's research PFAS library, was screened in DNT *in vitro* assays, which included the microelectrode array neuronal network formation assay (NFA)[39–41] and high-content imaging (HCI) assays to evaluate proliferation, apoptosis[42], and neurite outgrowth[43]. The DNT NAMs PFAS screening data were evaluated for: 1) possible bioactivity in DNT NAMs suggestive of effects on specific neurodevelopmental processes; 2) associations between PFAS physicochemical properties and structural feature descriptors with observed bioactivity; and 3) PFAS potency in the DNT NAMs compared to other chemicals and non-neural *in vitro* model systems.

Methods

Overview

This research effort includes new data for 160 PFAS that were tested in single-concentration (sc) and multiple-concentration (mc) response screening in a DNT NAMs battery comprised of the microelectrode array (MEA) network formation assay (NFA) and three different high-content imaging (HCI) assays measuring proliferation, apoptosis and neurite outgrowth (NOG). The chemical concentration-response data were normalized on a plate-by-plate basis to the median of the control wells and curve-fit using the ToxCast Pipeline (tcpl)[44]. PFAS bioactivity in the DNT NAMs was evaluated using several different approaches: 1)

hierarchical clustering of potency and efficacy to determine patterns of activity in distinct neurodevelopmental processes; 2) enrichment analysis of PFAS structure feature descriptors present in active PFAS; 3) cumulative frequency distribution of PFAS potency relative to all available PFAS chemicals screened in the DNT NAMs; and 4) potency comparisons of PFAS in DNT NAMs to non-neural *in vitro* model systems available in public data within ToxCast.

Chemical library

The PFAS tested in this study were procured by Evotec (US) Inc. (Branford, CT) under contract with the US EPA (Contract #EP-D-12–122 034). From an initial library of approximately 430 commercially available PFAS, PFAS were prioritized and selected for Tier 1 testing based on factors such as structural category, solubility in dimethyl sulfoxide (DMSO), and structural diversity to support read-across[45]. PFAS were deemed suitable for testing if they were soluble in DMSO above 5 mM, and lacking evidence of volatility or reactivity. For a complete list of procured PFAS see https://comptox.epa.gov/dashboard/chemical-lists/EPAPFASINV. There were multiple different PFAS procurements comprising the 160 PFAS screened, which included PFAS that were selected prior to and after analytical QC testing. See 'DNT NAMs screening' methods section for details on the screening approach of the two procurements. See Table S1 for chemical information on the 160 PFAS, their molecular formula, physicochemical properties, the analytical quality control (QC) results on the solubilized chemical stock samples, and the concentrations tested in the DNT NAMs battery.

Substances were solubilized in 100% DMSO at top stock concentrations of 30 mM if achievable without visible precipitation, with the exception of ammonium perfluoro-2-methyl-3-oxahexanoate (GenX), which was solubilized in H_2O as it was known to be unstable in DMSO[46]. For the vast majority of PFAS, mc screening concentrations ranged from 0.03 μM to 30 μM in the MEA NFA and 0.001 μM to 30 μM in the HCI assays in half-log increments, with a few exceptions (Table S1). Sc screening was performed at a target concentration of 30 μM, with a few exceptions based on solubility limitations. Two previously confirmed developmental neurotoxicants[47], i.e., methylmercuric(II) chloride[40] and tributyltin methacrylate[41], were used as comparator chemicals with known activity in the DNT NAMs and *in vivo*. All information on the chemicals and assays within the ToxCast chemical library are publicly available on the CompTox Chemicals Dashboard (https://comptox.epa.gov/dashboard) and within the ToxCast database, invitrodb version 3.5 (https://doi.org/10.23645/epacomptox.6062623.v8).

Quality Control (QC) analysis

Given the diverse physicochemical properties of the PFAS selected for this work and recent reports of instability of certain PFAS in DMSO[46], quality and stability evaluations were conducted of the PFAS screening stock solutions. Targeted analytical chemistry methods, specifically mass spectrometry coupled with either gas chromatographic or liquid chromatographic separation, were used to determine if the parent structure was present in the stock solution and to monitor for presence of degradants, contaminants, or isomers. A binary pass/fail grade was assigned for each stock[48]. A failing grade was based on several criteria,

including no analyte detected, analyte degraded, or incorrect molecular weight detected. Additional informational flags are listed in the README tab in the Supporting Information Tables. A QC fail grade indicates that the target PFAS was not present or was degraded and caution is recommended in interpreting bioactivity. Failure to observe bioactivity with QC-failed samples may not be interpretable as a true negative as we have no confirmation that the target PFAS analyte was present. Bioactivity observed with QC-failed samples suggests that bioactivity may have resulted from degradants or transformation products, and the concentration units reported are likely unreliable. Note that the QC analysis was performed on representative samples of the DMSO stock solutions and not directly from samples screened in the DNT NAMs.

Screening

The DNT NAMs dataset includes data from 160 PFAS that were screened in mc and/or sc from two chemical procurements: an original set selected prior to analytical QC testing and a re-procured set selected after preliminary QC testing (Figure S1). After initial DNT-NAM testing from the original procurement in mc and delivery of QC findings, application of a tiered screening approach was employed, leveraging a pre-screen in sc to evaluate activity before conducting a more resource intensive mc evaluation. Figure S1 describes the workflow, QC findings and number of PFAS for which activity was noted in the sc screening. To determine whether a chemical was active in at least one endpoint in the sc pre-screen, sc test well responses were normalized to the median of the control wells on a per-plate basis. The baseline median absolute deviation, or BMAD, was defined using the control wells and sc responses were considered active if they exceeded ± 2*BMAD, with a few exceptions. Additional details of sc analysis are in the Supporting Information Methods. Overall, this approach yielded datasets of 104 unique PFAS screened in mc MEA NFA, 57 PFAS screened in mc HCI assays, 56 PFAS screened only in sc MEA NFA, and 79 PFAS screened in only sc HCI assays.

DNT NAMs assays

See Carstens et. al (2022) for detailed experimental design for each assay. In brief, the MEA NFA was performed in a 48-well microelectrode plate format using rat cortical cells (dissected at P0 from Long Evans rat, (Charles River Laboratory, Raleigh, North Carolina)). Each chemical was screened in triplicate, with each replicate comprised of cells from multiple animals, across multiple plates. The data were collected over a period of 12 days *in vitro* (DIV) with recordings occurring on DIV 5, 7, 9, and 12. Chemical exposure started on DIV 0, two hours after plating, and full media changes occurred on DIV 5 and 9 (two repeat doses). The HCI assays were performed in a 96-well plate format using human neural progenitor cells (hNP1 cells derived from a neuroepithelial cell lineage of WA09 human embryonic stem cells, ArunA Biomedical (Athens, GA)) in the proliferation and apoptosis assays, human glutamatergic enriched neurons from iCell GlutaNeurons (derived from pluripotent stem cell, FUJIFILM Cellular Dynamics, Inc. (CDI) in the NOG assay). The length of the HCI assays ranged from 1–2 days with a single dose exposure occurring two hours after plating.

The MEA NFA includes 17 endpoints measuring decreased neuronal activity and two cytotoxicity endpoints[39–41]. The 17 MEA NFA endpoints were categorized into four 'activity types': general activity, bursting, network connectivity, and synchrony[49]. The HCI includes three assays: proliferation (2 endpoints)[42], apoptosis (2 endpoints), and NOG (4 endpoints)[43]. Each respective HCI assay includes a measure of cytotoxicity (highlighted gray in Table 1). The sc screening included a total of 14 endpoints: the 8 HCI endpoints listed above and a subset of 6 MEA NFA endpoints, which were selected as optimal based on their sensitivity and specificity to detect positive responses in mc screening. See Table 1 for a summary of endpoints included in the DNT NAMs battery. Also see Table S2A for a complete list of endpoints tested for each chemical and Table S2B for a summary of the mc or sc assays tested for each chemical.

Software

All data management, analysis, and figures were generated using the R statistical programming language within RStudio (version 4.1.2). All original code and source files for these analyses are available on GitHub (https://github.com/USEPA/CompTox-PFAS-DNT). Assay data were compiled using the ToxCast pipeline (tcpl) R package (version 2.1.0) that is publicly available (https://cran.r-project.org/web/packages/tcpl/index.html)[44], and these assay data are publicly available in the 'invitrodb' version 3.5 database (https://doi.org/10.23645/epacomptox.6062623.v8).

Data Pipeline

Chemical concentration-response data for each assay were normalized on a plate-by-plate basis to the median of the control wells and curve-fit using the tcpl to identify active or inactive chemicals[44]. Concentration-response data for each MEA NFA parameter were comprised of area under the curve measurements of time-response curves for each concentration, which included the four recordings (DIV 5, 7, 9, 12) over the multi-exposure experiment. The tcpl data processing methods and cutoff thresholds for a positive response for mc and sc endpoints are listed in Table S3. In general, baseline was defined as the baseline median absolute deviation (BMAD) of DMSO-treated wells. The cutoff threshold for a positive response in the mc screening endpoints was three times the BMAD for mc. Sc screening data presented in the results section were analyzed with a cutoff of three times the BMAD such that cutoffs were comparable with mc screening.

Seventeen MEA NFA parameters were fit in both the 'down' and 'up' activity direction. The endpoints measured in the 'up' direction were excluded from this analysis based on overall inactivity across the 17 endpoints and lack of positive control data for validation (Carstens et al. 2022). The HCI parameters were fit in the 'down' direction to capture a loss of bioactivity with the exception of "Casp3_7" (apoptosis). Examination of the HCI parameters fitted in the 'up' direction returned very little to no evidence suggesting increases in the assay parameters for functional processes. The proliferation endpoint "CCTE_Mundy_HCI_hNP1_Pro_MeanAvgInten_loss" was excluded from this analysis because the proliferation endpoint "CCTE_Mundy_HCI_hNP1_Pro_ResponderAvgInten_loss" was identified as more sensitive in an internal review of data.

Potency was evaluated in the mc screening data using the concentration at 50% maximal activity (AC_{50}) values. Sc screening methods were the same as described above.

Summary curve-fit information stored in level 5 of 'invitrodb' for mc data were used to filter chemical concentration-response curves to remove the least reproducible curve-fits from consideration as positives, with the following criteria[37, 50]: 1) curve-fits with ≥3 caution flags were set to a hit-call of zero (tcpl caution flags use both the plate level concentration-response data and modeled parameters to flag curve-fitting behaviors such as noisy data, only highest concentration above baseline, or hit-call potentially confounded by overfitting); 2) curve-fits with a top less than or equal to 1.2 times the cutoff for a positive and a resultant AC_{50} less than the concentration range screened were set to a hit-call of zero; 3) any hit-calls of −1, indicating the concentration series had fewer than 4 concentrations, was set to zero. When multiple samples of a chemical were available, a representative sample per chemical was identified using the library(tcpl) function 'tcplSubsetChid' which defaults to the most active and best quality curve available.

DNT NAMs Bioactivity Analysis

An 'active' chemical in the DNT NAMs battery was defined based on the following criteria. First, the set of AC_{50} values estimated by curve-fitting was filtered to retain *selectively* active concentration-response data (AC_{50} values occurring below the threshold of cytotoxicity). The threshold of cytotoxicity was defined as the AC_{50} value of the cytotoxicity endpoint from each respective assay. Selective DNT NAMs responses and cytotoxicity responses were used to characterize PFAS behavior as active or inactive in the DNT NAMs battery. Non-selective DNT NAMs responses were included when comparing PFAS bioactive concentrations to other non-DNT NAMs assays in ToxCast. The cytotoxicity endpoints included "MUNDY_HCI_CDI _NOG_NeuronCount_loss" for the NOG assay and "MUNDY_HCI_hNP1_CellTiter_loss" for the proliferation assay. The MEA_NFA contained two cytotoxicity endpoints ("CCTE_Shafer_MEA_dev_LDH_dn", "CCTE_Shafer_MEA_dev_AB_dn") of which the minimum log10-AC_{50} was computed in the case of two positive results. Second, a classification of 'active', 'inactive', or 'equivocal' was determined for each compound. An 'inactive' was defined as a chemical having no positive responses in the battery (mc or sc endpoints for chemicals that were not tested in mc screening). An 'active' was defined as any chemical that was positive in at least one endpoint (either in mc or sc endpoints for chemicals that were not tested in mc screening), unless the chemical was *only* active in one MEA NFA endpoint (not including the two cytotoxicity endpoints), in which case it was defined as 'equivocal'. This determination was based on previous findings that the MEA NFA endpoints are highly correlated and sensitive to chemicals with evidence of *in vivo* DNT[37]. For sc screening data, an equivocal was defined as a chemical with one positive response that was within 5% of the efficacy cutoff for any endpoint. In cases of binary classification of 'active' or 'inactive', an equivocal chemical was considered 'inactive'.

The potency of PFAS in the DNT NAMs was evaluated using several approaches, as follows: 1) The AC_{50} values were sorted into the different 'activity types' and the mean AC_{50} was computed for each group to determine the most sensitive 'activity type.' 2) Assay

endpoint sensitivity was evaluated by identifying which endpoints defined the minimum AC_{50} value for PFAS most frequently. 3) Unsupervised hierarchical clustering was used to evaluate the differential patterns of activity in PFAS screening in mc as measured by a metric that combines efficacy and potency, area under the curve (AUC). Not all PFAS that were screened in the MEA NFA were screened in the HCI assays; therefore, separate heatmaps were generated for each assay technology to visualize the data. These analyses used Ward's D2 method for linkage[51] (Ward, 1963) and the agglomerative clustering method as implemented in the R package 'gplots' version 4.1.3[52]) The distribution of PFAS potency values in the DNT NAMs was compared to the distribution of potency values for all available chemicals screened to-date in the same assay endpoints (415 total chemicals). An empirical cumulative distribution function was used to understand the percentage of PFAS with bioactivity above or below the median of potencies for all chemicals screened to date as well as the median potencies observed for the two chemicals with known *in vivo* DNT activity, i.e., methylmercuric(II) chloride and tributyltin methacrylate. The density of potency values for PFAS versus non-PFAS was used to understand whether PFAS behaved similarly to non-PFAS with respect to potency in the DNT NAMs. 5) PFAS potency in the DNT NAMs was compared to two other NAMs in the ToxCast screening program (https://doi.org/10.23645/epacomptox.6062479.v5) – the BioMAP® Diversity PLUS panel and the Attagene cis-Factorial and trans-Factorial assays – with the goal of identifying substances with neural-specific effects. The BioMAP® Diversity PLUS panel is a phenotypic screening platform of primary human cell co-culture systems that is comprised of 12 assays, encompassing 148 endpoints, modeling diverse tissue and organ systems (particularly vascular and immune biology)[53–54]. The Attagene cis-Factorial and trans-Factorial assays are two multiplexed high-throughput screening assays that use HepG2 cells to assess transcriptional factor activity (cis-Factorial) or transfected nuclear receptor activity (trans-Factorial) that encompass 69 biological endpoints[55–56].

PFAS chemical and structure feature descriptors

Trends in physicochemical properties and structure feature descriptors and DNT NAMs bioactivity were examined using several approaches. The relationship between three chemical properties (the perfluorinated carbon chain length (CF chain length), the C: fluorine (F) ratio, and logP) and PFAS activity was evaluated using a Student's unpaired t-test for significance ($p < 0.05$). The CF chain length was binned into three groups <4, 4:7 C, and ≥8 C atoms and differences in percent activity ('number of active responses'/ 'total number of endpoints tested' * 100 per chemical) per bin were evaluated. A database framework to facilitate structural category assignment of PFAS referred to as 'PFAS-Map' developed by Su and Rajan (2021) was used to profile the PFAS into nominal OECD[57] chemical structure categories[58]. Further details of how these have been used to profile other PFAS lists on the Dashboard and how these related to the PFAS tested are discussed in Patlewicz et al., in prep. Su and Rajan (Su and Rajan 2021) implemented PFAS-Map as an open-source tool (https://github.com/MatInfoUB/PFAS_Map_MaDE_UB) that enables large numbers of PFAS to be objectively and systematically profiled into at minimum 9 broad OECD categories. These PFAS-Map OECD categories were also related to percent activity. Correlations between mean AC_{50} values by chemical and physicochemical properties (C:F ratio, CF chain length, logP, molecular weight, boiling point, and vapor pressure) were

examined using linear regression modeling, using correlation coefficients (R) with p-values for significance ($p < 0.05$) to understand the significance of these linear relationships. Physicochemical and environmental fate properties were extracted from the CompTox Chemicals Dashboard (https://comptox.epa.gov/dashboard), including predicted properties from the OPEn structure–activity/property Relationship App, or OPERA[59–60].

The structure feature descriptors employed herein are two dimensional descriptors based on the approach used to develop the original ChemoType ToxPrints [61](Yang et al., 2015). An initial set of PFAS ToxPrint categories were defined by visual inspection of ToxPrints relative to the expert assigned structural categories used in the selection of the PFAS for testing[45, 62]. A subset of 34 categories, denoted TxP_PFAS_34cat, were derived, either from single ToxPrints or Boolean combinations of ToxPrints, that were able to group the vast majority of the ~150 PFAS. These included ToxPrints representing isolated functional groups, such as primary alcohols, sulfonic acids etc., as well as a few PFAS-specific ToxPrints, such as perfluoro-propyl, -butyl, -hexyl, and -octyl chains. Note that the PFAS ToxPrint category 'PFAS_perFoctyl' is identical to the public ToxPrint 'bond:CX_halide_alkyl-F_perfluoro_octyl'. The PFAS-specific ToxPrints were uploaded into the ChemoTyper software (Version 1.0), an application that allows for searching and highlighting chemical substructures (https://chemotyper.org/). Chemical structure information of the set of 160 PFAS was extracted from the ACToR-DSSTox Chemical Registration (https://ccte-chemreg.epa.gov/ChemReg/export.jsf) using the 'Download DSSTox Substructures (v2000)' function. This file was uploaded into the ChemoTyper software and matched to the PFAS-specific ToxPrints. Chemical 'fingerprints,' a binarized classification of the ToxPrints for each chemical, were extracted. A ToxPrint enrichment analysis[50, 63] was performed to determine the likelihood that a particular ToxPrint is represented in the set of active PFAS for DNT NAMs (versus the inactive PFAS set) more frequently than would be predicted by chance. ToxPrints that were not represented in at least 3 PFAS or that were represented in all PFAS were removed prior to calculating enrichment. The statistical thresholds for significant enrichment included an odds ratio of ≥ 3 and a Fisher's exact p-value of < 0.05.

Results

PFAS bioactivity and sensitivity by neurodevelopmental process

A total of 160 unique PFAS, representing distinct PFAS-Map OECD structural categories (Figure S2), were screened in sc and/or mc DNT NAMs comprised of four assays representing four key neurodevelopmental processes: neural network formation measured by the MEA technology and proliferation, NOG, and apoptosis measured by the HCI technology. A subset of 74 chemicals were screened in only mc MEA NFA, while a subset of 136 chemicals were screened with a tiered screening approach whereby active chemicals in sc screening were subsequently screened in mc (Figure S1).

A key observation of this screening was that the majority of PFAS were inactive in the DNT NAMs battery: 111/160 PFAS demonstrated no positive responses across the DNT battery, including PFOS, PFHxS, PFHxA, PFBS, and GenX, and 7/160 were determined to be equivocal, including PFOA and PFHpS (Table 2). PFOA bioactivity was classified as

'equivocal' given that it was active in only 1/17 mc MEA NFA endpoints, not including cytotoxicity. PFHpS was classified as an 'equivocal' because it was only positive in one sc endpoint measuring decreased proliferation, screened at a concentration of 20 μM, and had efficacy below the cutoff by less than 5%.

Analytical quality control (QC) analysis was performed on PFAS stock solutions in DMSO to evaluate purity and stability and provide context for interpreting bioactivity data. Of the 118 inactive or equivocal PFAS in the DNT NAMs, 43 failed QC testing, as such, the PFAS that were inactive or equivocal and also failed QC may have been inactive because the samples were not stable or amenable to screening in aqueous assay technologies such as those employed herein. The majority of QC flags for PFAS with no DNT bioactivity were due to analyte degradation or no sample detected (see Table S4 for complete list of PFAS bioactivity and QC results). Of the 42 PFAS that were positive, 10 failed QC testing; for these PFAS, bioactivity may have resulted from uncharacterized metabolites and/or degradants. The QC pass/ fail results appeared associated with several physicochemical properties (Figure S3). PFAS that failed QC typically demonstrated lower values for molecular weight, octanol:water partitioning coefficient (logP), and boiling point, as well as a higher vapor pressure, compared to PFAS that passed QC (Student's t-test, $p < 0.01$).

PFAS bioactivity in the DNT NAMs was evaluated for each assay (MEA NFA, NOG, proliferation, apoptosis, and cytotoxicity). In this analysis, only the positive responses below the threshold of cytotoxicity (the cytotoxicity AC_{50} for each chemical in each assay) were evaluated for the MEA NFA, NOG, proliferation and apoptosis assays. PFAS demonstrated the most bioactivity overall in the assay measuring neural network formation compared to other DNT assays, with 32/160 PFAS active in at least one endpoint in the sc or mc MEA NFA, of which six were considered equivocal in the sc or mc MEA NFA Figure 1A). Cytotoxicity was observed for 23/160 PFAS active in at least one cytotoxicity endpoint, including five different measurements of cell health (neuron count number in hNP1 and CDI cells, ATP content in hNP1, or mitochondrial function and plasma membrane permeability in rat cortical cells). Only 15/132 PFAS demonstrated activity in the assay measuring neurite outgrowth, which measured decreases in length of developing neurites, number of total neurites, and number of branch points. The proliferation and apoptosis assays detected the least bioactivity, with 8/136 or 1/136 active PFAS, respectively. Note that the only active PFAS in the apoptosis assay, 3H-Perfluoro-2,2,4,4-tetrahydroxypentane, failed QC testing with a flag for no sample detection. Although this compound was active in one other endpoint measuring cytotoxicity, 'MEA_dev_LDH_dn', at a comparable potency (1.32 log10-μM versus 1.03 log10-μM, respectively), the bioactivity should be interpreted with caution as it may have resulted from uncharacterized degradant(s). These data suggest that neural network formation is the most sensitive neurodevelopmental process to perturbation by PFAS, whereas proliferation and apoptosis are the least sensitive.

The potency of PFAS bioactivity was compared across different types of activity in the DNT battery. The 17 endpoints comprising the MEA NFA were further categorized into four different types of neuronal activity: general activity, bursting, network connectivity, and oscillatory[49]. The mean potency of all active hits in the mc screening battery was 0.68 ± 0.53 log10-μM (log10-AC_{50} ± SD; Table S6A for the log10-AC_{50} for each chemical

by endpoint). The endpoints measuring 'general activity' in the MEA NFA demonstrated the most potent bioactivity overall (mean ± SD of 0.52 ± 0.54 log10-μM) (Figure 1B). The mean potency of 'general activity' endpoints was less than the mean potency of 'cytotoxicity', 'NOG', and 'oscillatory' activity types (one-way ANOVA, Tukey's multiple comparison, $p<0.05$, Table S6B). There were six potent outliers (< 0.5 log10-μM) that were captured by the MEA NFA, of which four failed QC testing and two were equivocal, indicating low confidence in the bioactivity. Given the trend in potent activity in the MEA NFA, we evaluated assay endpoint sensitivity by identifying which endpoints determined the minimum AC_{50} value for each compound. The MEA NFA 'general activity' endpoint measuring a decrease in the number of bursting electrodes and the NOG endpoint measuring a decrease in neurite length were the most sensitive overall (Figure S4Ai). Given the high frequency of chemicals associated with the endpoint measuring a decrease in the number of bursting electrodes relative to other endpoints, the concentration response curves for the eight positive responses in this group were evaluated (Figure S4B). Seven out of eight curves demonstrated 'high confidence' bioactivity, whereas one positive response from perfluoroglutaryl difluoride was equivocal and failed QC testing (see Figure S4C for more details). Excluding this one equivocal response, the average minimum potency captured by this endpoint was 0.20 log10-μM ± 0.63 (mean AC_{50} ± SD), in contrast to 1.08 log10-μM ± 0.43 (mean AC_{50} ± SD) for the endpoint measuring a decrease in neurite length. The endpoint 'bursting_electrodes_number_dn' also ranked as the most potent endpoint overall when comparing the mean AC_{50} by endpoint for all positive responses from the 74 mc-screened PFAS (Figure S4Aii). Together, these results indicate that the endpoint measuring a decrease in the number of bursting electrodes appears to be particularly sensitive to perturbation by PFAS.

PFAS efficacy in the DNT NAMs

Of the 160 PFAS that were screened in the MEA NFA, 29 PFAS demonstrated potent and efficacious activity in the MEA NFA that was selective, as illustrated by hierarchical clustering of AUC values computed for each chemical-by-endpoint curve (Figure 2). Clustering of PFAS revealed three main clusters of differential patterns of efficacy (rows/y-axis dendrogram) across five activity types (column bar legend) that are compared to tributyltin, a chemical with known DNT effects *in vivo*: cluster 1) four PFAS with moderate efficacy and bioactivity across all four neuronal activity types (mean AUC ±SD of 78.9 ± 15.5); cluster 2) six PFAS with moderate efficacy and bioactivity in mainly endpoints measuring network connectivity and a lack of bioactivity in 'general activity' endpoints measuring mean firing rate and burst rate (mean AUC ±SD of 39.7 ± 17.1); cluster 3) 19 PFAS with moderate or low activity in a targeted subset of variable endpoints (mean AUC ±SD of 7.83 ± 6.37) with a sub-cluster of four chemicals driven by common activity in the mutual information endpoint and some activity in network connectivity endpoints (dotted line); and cluster 4) tributyltin with high efficacy across the majority of endpoints with a mean AUC of 260, a fold-difference of 3.3 times greater than the most potent and efficacious PFAS in cluster 1, indicating that overall, the subset of 29 bioactive PFAS were markedly less potent and efficacious relative to a DNT NAMs-active compound with evidence of *in vivo* DNT. Of the 19 PFAS in cluster 3, two failed QC testing (red row labels), and four were classified as demonstrating equivocal bioactivity (asterisk after row label), including

PFOA (see Figure S5 for the PFOA concentration response curve). In cluster 2, one PFAS failed QC, 2,2,3,3-tetrafluoropropyl acrylate, with a flag for evidence of analyte degradation. PFAS containing a perfluorinated C chain length (CF chain length) of 8:14 C predominantly grouped in the higher bioactivity clusters 1 and 2 (Figure 2, left row side legend). PFAS in clusters 1 and 2 were also comprised of five shorter CF-chain PFAS, three of which contained a carboxylic ester acrylic functional group. However, there were no clear trends in PFAS-Map OECD structural categories and ranking PFAS by the AUC sum (Figure S6), possibly due to the limited representation of all the PFAS-Map OECD structural categories among the PFAS that were selectively active in the MEA NFA (Figure S2).

Of the 57 PFAS screened in the mc HCI assays, 12 were active in the NOG mc assay and one was active in the mc apoptosis assay, demonstrating low efficacy and/or potency compared to the DNT NAMs-active compound tributyltin (Figure S7). The average AUC of tributyltin across the HCI assay endpoints was 38.4 times greater than the average AUC of the 13 PFAS that were active in the HCI assays (135 compared to 3.52 ± 2.66 (± SD), respectively). None of the PFAS were active across multiple HCI assays and upon inspection of the concentration response curves, the majority of curves demonstrated activity only at the highest concentration tested and/or efficacy levels less than 50% (Figure S8), indicating that the PFAS bioactivity is neither potent nor efficacious in the HCI assays. There was no clear trend in the CF chain length and the AUC values in the HCI assays. Of the PFAS that were tested in the HCI assays, 37 were also screened in the mc MEA NFA, of which only four were active in both the MEA NFA and at least one HCI assay: 2-(perfluorooctyl)ethanol, flubendiamide, 11:1 fluorotelomer alcohol, and perfluorooctanamidine. Conversely, of the 29 PFAS that were active in the MEA NFA, 17 were tested in the HCI assays, of which only the four above-mentioned PFAS were active in at least one HCI endpoint. These results suggest that PFAS demonstrating efficacy in the HCI assays measuring NOG, proliferation or apoptosis do not necessarily predict similar perturbations in the MEA NFA, and vice versa. Overall, PFAS appear to show greater overall efficacy and potency in the MEA NFA compared to activity in the NOG, proliferation, or apoptosis assays (mean AUC ±SD of 24.5 ± 28.8 in the MEA NFA compared to mean AUC ±SD of 3.52 ± 2.66 in the HCI assays).

Trends in PFAS chemical and structure feature descriptors

We next evaluated trends between chemical or structure feature descriptors and activity in the DNT NAMs battery. Here we compared PFAS sc and mc screening activity in the DNT NAMs battery to the C: fluorine (F) ratio, CF chain length, and logP. The C:F ratio and lopP were identified as properties that were increased in active PFAS compared to inactive PFAS (Figure 3A, Student's unpaired T-test for significance, $p < 0.05$). The relationship of the CF chain length and DNT NAMs activity was further examined by comparing the percent activity of each PFAS to the CF chain length in three bins: <4 C, 4:7 C, or ≥8 C (Figure 3B). Qualitatively, this analysis revealed that active PFAS with ≥8 C demonstrated the highest percent activity in the DNT NAMs compared to 4:7 C and <4 C, which demonstrated the lowest percent activity as measured by the median percent activity of active PFAS. Evaluating PFAS-Map OECD structure categories and percent activity did not reveal any clear trends (Figure 3C). Correlations between chemical properties (C:F ratio, CF chain

length, logP, molecular weight, boiling point, and vapor pressure) and mean AC_{50} values by chemical from mc screening data were examined using linear regression modeling and revealed no significant correlations ($p>0.05$, Figure S9). These results suggest that PFAS containing a longer CF chain length, particularly a CF chain length of ≥ 8, and a higher C:F ratio may correspond to higher DNT NAMs positive hit rates.

We performed a ToxPrint enrichment analysis, which determines the likelihood that a particular ToxPrint (a public set of chemotypes, http://www.toxprint.org) is overrepresented in the active PFAS set compared to inactive PFAS set in the DNT NAMs. Of the 74/729 public ToxPrints that met the inclusion criteria, no ToxPrints were significantly enriched (Table S7); however, after excluding PFAS that failed QC testing, two ToxPrints containing a carboxylic acid moiety were significantly enriched ($p < 0.05$ and odds ratio ≥ 3) (Table S8). A list of 34 expert curated PFAS specific ToxPrint categories (TxP-PFAS_34cat) (Table S9)[62] were assigned to each chemical in this study. Following the same criteria described above, 28/34 PFAS ToxPrints met the inclusion criteria and none were significantly enriched in active PFAS (Table S10), however after excluding the PFAS that failed QC testing, 21/34 PFAS ToxPrints met the inclusion criteria, and one ToxPrint containing a carboxylic acid moiety was enriched by significance (Table S11). Evaluating the 34 PFAS ToxPrints by percent activity in the DNT NAMs revealed that PFAS containing a sulfonamide, acrylate, or perFoctyl (a CF chain length ≥ 8) moiety demonstrated the highest activity, as qualitatively determined by the mean percent activity of active PFAS per ToxPrint (Figure 3D). Non-PFAS chemicals containing carboxylic acid or sulfonamide moieties were not more likely to be active in the DNT NAMs based on a ToxPrint enrichment analysis of all available chemicals screened in the DNT NAMs (Table S12). This analysis also revealed five PFAS ToxPrints comprising inactive PFAS. A larger dataset including PFAS representing overlapping and diverse functional groups would improve the interpretation of this analysis.

Comparison of PFAS potency in the DNT NAMs to other chemicals and assays

We next compared the potency and efficacy range of all PFAS tested to all available chemicals screened in these assay endpoints in the ToxCast database. This dataset was comprised of 415 chemicals, including some known to cause developmental neurotoxicity *in vivo*[47], tested in a concentration range of - 1.81 to 1.44 log10-μM with a few exceptions. In comparing the AC_{50} values of PFAS to all available chemicals in the DNT NAMs, the median potency of active PFAS chemicals was near the median of all chemical potencies in DNT NAMs (Figure 4A). Compared to two known neurodevelopmental toxicants, the median potency for PFAS (median ± SD of 0.87 ± 0.52 log10-μM) was 1.40 log10-μM greater than the median potency of methylmercury (median ± SD of −0.53 ± 0.48 log10-μM) and 2.3 log10-μM greater than the median potency of tributyltin (median ± SD of −1.40 ± 0.49 log10-μM) in the DNT NAMs. The minimum 5th percentile potency of PFAS was less potent than the median potency of methylmercury and tributyltin. Relative to all non-PFAS chemicals, few PFAS demonstrated bioactivity below 1 μM (Figure 4B). These results indicate that the majority of PFAS bioactivity occurs within a similar potency range as non-PFAS chemicals and was several orders of magnitude less potent than two known neurodevelopmental toxicants in the DNT NAMs. Moreover, the efficacy of PFAS, as measured by the median AUC sum per chemical, approached the 25th percentile of AUC

sum values from all available chemicals and the 95th percentile of PFAS AUC sum was less than the median AUC sum of both methylmercury and tributyltin (Figure S10). These results indicate that PFAS are generally less efficacious than a majority of non-PFAS chemicals and markedly less efficacious than two neurodevelopmental toxicants by several orders of magnitude.

Next, we compared DNT NAMs bioactivity to two other NAM assays in the ToxCast screening program[64], the BioMAP® Diversity PLUS panel[65] and the Attagene cis-Factorial and trans-Factorial assays[55], with the goal of identifying substances with specific responses in the DNT NAMs. Twenty-one of the 99 PFAS screened in all three mc assays were active in all three mc assays, of which 16 were more potent in the mc DNT assay battery compared to both the Attagene and BioMAP assays, as measured by the mean AC_{50} value across all active endpoints in each assay (Figure 5A). Five PFAS exhibited activity in *only* the mc DNT assays, of which four were active in only one mc HCI endpoint and the other was active in only two mc MEA NFA endpoints. Moreover, of the 68 PFAS that were *inactive* in the mc DNT assays, 54 were active in the Attagene or BioMAP assays (Figure S11A), indicating fewer PFAS perturbed the DNT NAMs compared to the Attagene and BioMAP model systems. 1H,1H,8H,8H-perfluorooctane-1,8-diol demonstrated the lowest mean potency in the DNT NAMs, which was approximately 1.5 log10-μM more potent than the mean potency in the Attagene and BioMAP assay. Four PFAS were more potent in the BioMAP assay compared to the DNT assay, notably 11:1 Fluorotelomer alcohol which was 1.5 log10-μM more potent than the DNT mean potency and 2.5 log-fold more potent than the Attagene mean potency (Figure 5B). Given that the majority of PFAS were more potent in the DNT NAMs relative to the Attagene and BioMAP assays (Figure S11B), we evaluated whether this trend was common for any set of non-PFAS chemicals screened in all three assays. We found that DNT NAMs potencies were significantly decreased relative to BioMAP and Attagene potencies (mean ±SD of 0.61 log10-μM ± 0.91 in the DNT NAMs compared to 1.12 log10-μM ± 0.87 and 1.13 log10-μM ± 0.53 in the BioMAP and Attagene assays, respectively, $p<0.0001$, Welch two sample t-test, Figure S11C). Based on this finding, we cannot conclude that PFAS disrupt neural systems at a more potent concentration compared to other *in vitro* biological targets. In conclusion, this analysis revealed that PFAS bioactivity was unlikely to be neural-specific given that few PFAS was active in the DNT NAMs that were not active in the BioMAP and Attagene assays and that a majority of PFAS were inactive in the DNT NAMs but active in the other two assays.

Lastly, we identified the PFAS with the highest bioactivity in the DNT NAMs battery. Highly active PFAS were defined as PFAS that were active in greater than 30% of tested endpoints. Recently we reported that bioactivity in the DNT NAMs is highly correlated across endpoints such that chemicals with evidence of *in vivo* DNT were more likely to be active across multiple endpoints in the DNT NAMs[37]. We identified 11 PFAS that were highly active in the DNT NAMs (Table 3), of which one failed QC testing, 2,2,3,3-Tetrafluoropropyl acrylate, with a flag for evidence of degraded analyte (in some instances due to DMSO). Interestingly, this chemical also contained the lowest CF chain length of only 2 but a high C:F ratio of 1.5. Of the highly active PFAS, 6/11 had a CF chain length of ≥ 8 and the remaining PFAS had a C:F ratio ≥ 1. The most active PFAS, N-[(perfluorooctylsulfonamido)propyl]-N,N,N-trimethylammonium iodide, contained three

different moieties: sulfonyl, sulfonamide, and perFoctyl (a CF chain length ≥ 8). Of the five most active PFAS, three included a perFoctyl moiety, two included an acrylate moiety, one included an oxidehydroxy moiety, and two included the combination of sulfonyl, sulfonamide, and perFoctyl moieties. These data indicate that PFAS with a CF chain length of ≥ 8 are associated with increased DNT NAMs bioactivity and that particular functional groups, such as sulfonamide, sulfonyl, and acrylate, may also be implicated in elevated DNT NAMs bioactivity.

Discussion

This work presented novel data collection and results of an integrated analysis of concentration-response data for 160 PFAS screened in a DNT NAMs battery evaluating key neurodevelopmental processes, proliferation, apoptosis, neurite outgrowth, and neural network formation and function[39–41, 66]. The majority of screened PFAS (118/160) were inactive (111) or equivocal (7) in the DNT NAMs battery, of which 43 failed to be identified as present in analytical quality control stock samples. Of the 42 active PFAS, 32 were verified as present by analytical quality control and demonstrated bioactivity in endpoints measuring decreases in neuronal network function or neurite length. Structural feature descriptors such as a CF chain length of ≥ 8, a high C:F ratio, or PFAS containing moieties, such as carboxylic acid, sulfonamide and acrylate, were identified as associated with PFAS bioactivity in the DNT NAMs. PFAS were notably less efficacious in the DNT NAMs compared to all available chemicals screened in the DNT NAMs, and the median PFAS potency was less than the median potency of two known *in vivo* developmental neurotoxicants by several orders of magnitude. Lastly, PFAS that were active in the DNT NAMs were also active in other NAM assays. Taken together, these observations indicate PFAS demonstrated low efficacy and potency in the DNT NAMs and may not demonstrate neural specific effects based on comparisons with non-neural NAM assays.

Given the widespread commercial and industrial applications of PFAS, current research is focused on understanding important aspects of PFAS in our environment, such as their chemical stability, persistence, bioaccumulation, and their potential for human hazard. Of particular interest is neurodevelopmental outcomes of PFAS exposure during vulnerable stages of development[67]. Epidemiological studies have examined associations between prenatal exposure to PFAS, particularly PFOS and PFOA, and higher impulsivity and increased ADHD prevalence but results are inconclusive[19]. A subset of PFAS have been detected in nervous tissues of human, diverse taxa of exposed wildlife, and in experimentally exposed laboratory animals[11, 13]. Animal studies provide evidence that prenatal exposure to PFOS or PFOA can elicit DNT effects[12]. A single oral exposure of 21 μM/kg PFOS or PFOA at postnatal day (PND) 10 in mice was found to cause hyperactivity and habituation deficits at 2 and 4 months of age and changes in cholinergic markers[32–33]. Offspring of mice exposed to 3 mg/kg/day PFOS (6 μM) during gestation displayed more intense and disorganized spontaneous activity[68] or anxiety-like phenotype[35]. Similarly, zebrafish exposed to PFOS from 0–6 days post fertilization (dpf) displayed a disorganized pattern of spontaneous activity (1.86 μM)[69] and hyperactivity phenotype (3.1 μM PFOS) [70]. We found PFOS was inactive in the DNT NAMs battery and PFOA was equivocal (positive in 1/27 endpoints), screened at an upper concentration of 40 μM (2.0×10^4 μg/L) and 30

μM (1.2×10^4 μg/L), respectively. Both PFOS and PFOA were successfully detected in analytical QC of stock solutions. Testing at higher concentrations may not be relevant to human exposure. Serum levels from 3–5 year old children in the U.S. population measured concentrations of 3.75 μg/L PFOS and 1.94 μg/L PFOA (2013–2014 National Health and Nutrition Examination Survey)[71], concentrations that were more than five thousand fold less than the maximum concentrations screened in the DNT NAMs and more than five hundred fold less than the lowest effect level observed in animal DNT studies.

The majority of screened PFAS were inactive or equivocal in the DNT NAMs battery (118/160). Of the 49 PFAS that were positive in at least one endpoint, 32 PFAS were positive in ≤ 2 endpoints. Recently we reported that bioactivity in the MEA NFA is highly correlated across endpoints, such that chemicals were more likely to be active across multiple endpoints[37]. We are therefore cautious about the interpretation of bioactivity in only a single MEA NFA endpoint, such as in the case of PFOA. Two endpoints measuring neuronal network connectivity and neurite length were particularly sensitive to PFAS perturbation. The endpoint measuring a decrease in the number of bursting electrodes was the most sensitive MEA NFA endpoint, which is in contrast to our recent study that identified the mutual information endpoint as the most sensitive endpoint for a subset of 92 chemicals screened in the DNT NAMs battery, including 53 chemicals with evidence of *in vivo* DNT effects[37]. Seven out of the eight positive responses in the endpoint measuring decreased number of bursting electrodes demonstrated 'high confidence' bioactivity, affirming that this endpoint may be particularly sensitive to perturbations by PFAS. The NOG endpoint measuring a decrease in neurite length was the most sensitive endpoint among the HCI assays to perturbations by PFAS, however, upon manual review of concentration response curves, we found that positive responses in the neurite length loss endpoint were low efficacy and demonstrated activity only at the highest concentration tested. We therefore conclude that the NOG assay, similar to the apoptosis and proliferation assays, is largely insensitive to perturbation by PFAS with the most sensitive bioactivity occurring at high concentrations (30 μM). In the future, PFAS should be screened in additional DNT NAMs that model neurodevelopmental processes that are not currently represented in this battery to determine whether other assays may be more sensitive to PFAS exposure.

In examining the 160 PFAS screened herein, it was important to understand if certain subsets of PFAS may correspond to higher likelihood of bioactivity, as the list of unique PFAS may be in the thousands. We identified PFAS containing a carboxylic functional group as more likely to be active and PFAS containing a sulfonamide, acrylate, and perFoctyl (≥ 8 CF chain length) moieties as highly active in the DNT NAMs.. Recent work identified associations between PFAS structural features, such as the C chain length, the degree of fluorination and functional groups, and PFAS toxicity in the brain[72–74]. Gaballah et al. (2020) found that developmental exposure to long-chain PFAS in zebrafish was associated with a hyperactivity phenotype. PFAS with longer C chain-length were associated with increased neuronal activity in rat hippocampal neurons[72]. Interestingly, several zebrafish studies report greater developmental toxicity potential from PFAS containing a sulfonate functional group compared to carboxylic acid functional group[70, 73–74]. In the DNT NAMs, PFAS containing a sulfonamide were more active compared to PFAS containing carboxylic acid as measured

by percent activity (median of 49.3% activity versus 7.14% activity). The rationale for why particular functional groups may be more active in DNT NAMs is unclear. Our observation that PFAS with carboxylic acid or sulfonamide moieties were more likely to be bioactive in DNT NAMs is consistent with this previous NAMs study (Houck et al 2021) and with the use of these moieties in the development of bioactive pharmaceutical drugs[75–77]. A recent study evaluated a structurally diverse set of PFAS, largely overlapping with the library evaluated herein, and found that PFAS that interacted with nuclear receptor targets contained functional groups with negative ionic charge at physiological pH, consistent with known critical components for ligand-binding[55]. Screening more representative PFAS that contain these diverse functional groups would increase certainty in the associations between functional groups and increased bioactivity of PFAS.

Several limitations should be considered in the interpretation DNT NAMs bioactivity for predicting *in vivo* DNT potential. PFAS structural feature descriptors and physicochemical properties such as longer perfluorinated carbon chains, ionization at neutral pH, and higher octanol:water partitioning, are thought to contribute to PFAS bioaccumulation potential *in vivo*[78–79] and may also increase cellular bioavailability in *in vitro* assays. PFAS with greater than 10 C atoms had the highest bioaccumulation in the brain of North Atlantic pilot whales[14], however it is unclear whether bioaccumulation potential indicates toxicity potential. Several transporter proteins, serum albumin, and organic anion transporters have been reported to play a vital role in regulating the pharmacokinetics of PFAS[80–82], which may affect the activity of these PFAS *in vivo,* but are not fully present in the DNT NAMs applied herein that lack a serum compartment and blood brain barrier. However, some of the same characteristics that are thought to contribute to PFAS bioaccumulation may also influence *in vitro* disposition, such as binding to serum proteins or plastics, and consequently impede cellular bioavailability. In addition, metabolism is a critical component of the toxicokinetics of PFAS that should be considered in the interpretation of DNT NAMs activity. Xenobiotic-metabolizing enzymes in the DNT NAMs models are relatively uncharacterized and are likely to differ from those in other tissues[83]. These differences may be key factors with unknown consequences regarding PFAS inactivity observed across the DNT NAMs.

Out of the 118 inactive or equivocal PFAS, 43 failed analytical QC of stock samples and 32/42 active PFAS were successfully detected in QC. These data suggest that the 43 inactive PFAS maybe not be true negatives in the DNT NAMs battery. QC flags provided rationale for why a chemical may not be present in analytical quality control of the stock samples. A majority of PFAS with the “Fns” flag (no sample detected) were those with low boiling points or high vapor pressure. For chemicals in this group that were not active in the DNT NAMs battery, the speculation is that these might have volatilized prior to or during the NAM assay. For the chemicals in this group that were active in the DNT NAMs, the issue might be that the chemical was not detected on the analytical instrumentation because of the temperature requirements in the mass spectrometer source required to ionize them. It is important to note that failure to detect a specific analyte does not necessarily mean that a chemical is not present in the stock. Rather, given the detection strategies employed, inability to detect an analyte might indicate that further analytical assessment is necessary. For example, allyl perfluoroisopropyl ether failed to be detected in analytical quality control

of the stock sample but was active in 3/19 mc DNT NAMs endpoints, which suggests that the chemical may not have been present in the mass spectrometer, likely due to its low boiling point (OPERA predicted BP of 76.3°C), but some amount could have been present under assay conditions.

PFAS potency comparisons in the DNT NAMs battery indicated that PFAS potency on average was similar to the potency of non-PFAS chemicals screened in the DNT NAMs battery and was less potent than two chemicals known to have *in vivo* DNT effects and that are active in the DNT NAMs. PFAS efficacy comparisons, as measured by AUC, indicated that PFAS efficacy was lower than non-PFAS chemicals screened in the DNT NAMs battery. The list of non-PFAS chemicals consists of chemicals with and without evidence of *in vivo* DNT hazard, including metals, pesticides, neuroactive and non-neuroactive drugs, and negative reference chemicals. These data suggest that the neurodevelopmental processes evaluated in this battery are less sensitive to PFAS in comparison to two chemicals with evidence of *in vivo* DNT hazard [84–85]. Interestingly, PFAS DNT bioactivity was more potent on average than PFAS bioactivity in two other non-neuronal *in vitro* NAMs, the BioMAP and Attagene assays. These two assays evaluate vascular, immune, or transcriptional regulation model systems, suggesting that neuronal systems may be more sensitive to perturbations by PFAS than other biological systems. However, we also demonstrate that potencies of non-PFAS chemicals were left-shifted in the DNT NAMs compared to BioMAP and Attagene assays. One methodological explanation for the potency difference may be exposure duration. The MEA NFA involved a 12-day chemical exposure period with two repeat doses; in contrast the BioMAP and Attagene assays involved a single dose over a 24 hour to 6-day exposure duration. These data suggest that the lower potency in the DNT NAMs relative to other NAMs may be explained by repeat dosing and longer *in vitro* exposures; however, these differences require further investigation.

Conclusion

The paucity of experimental data evaluating a large number of PFAS is a discernable limitation in understanding human health effects of PFAS in the developing brain. Given the challenges of interpreting the DNT potential of PFAS in the environment from human epidemiology studies, alternative approaches are needed to evaluate the effects of PFAS exposure on adverse neurodevelopmental outcomes. This novel analysis demonstrates the power of using high-throughput screening and computational approaches to integrate a broad battery of DNT NAMs assays representing key neurodevelopmental processes. We found that a subset of 160 PFAS representing six distinct PFAS-Map OECD structural categories were largely inactive in the DNT NAMs and that a subset of PFAS demonstrated relatively high potency and low efficacy. We found that the majority of DNT NAMs-active PFAS were also active in other NAMs and that DNT NAMs potencies were decreased relative to other NAMs. Importantly, our findings support *in vivo* studies that report an association between PFAS containing a longer CF chain length or carboxylic acid or sulfonamide functional groups and elevated DNT potential based on *in vitro* NAM results. Additional screening including PFAS representing overlapping and diverse functional groups and analysis of toxicokinetic parameters will be important for improving the interpretation of the DNT potential posed by these chemicals.

Supplementary Material

Refer to Web version on PubMed Central for supplementary material.

Acknowledgements

The authors would like to acknowledge Dr. Michael Devito and Dr. Richard Judson at the US Environmental Protection Agency for insightful comments on previous versions of this manuscript.

Funding

The United States EPA, through its Office of Research and Development, provided funding for this research. A.C. and S.C were supported by appointments to the Research Participation Program of the USEPA, Office of Research and Development, administered by the Oak Ridge Institute for Science and Education through an interagency agreement between the U.S. Department of Energy and the USEPA.

Abbreviations

AB	Alamar Blue
AC_{50}	concentration at 50% maximal activity
AED	administered equivalent dose
AUC	area under the curve
CDI	Cellular Dynamics International
DIV	day *in vitro*
DMSO	dimethyl sulfoxide
DNT	Developmental neurotoxicity
EPA	[United States] Environmental Protection Agency
HCI	high content imaging
hNP1	human neural progenitor cells derived from a neuroepithelial cell lineage of WA09 human embryonic stem cells, ArunA Biomedical (Athens, GA)
LDH	lactate dehydrogenase
mc	multi-concentration
MEA	microelectrode array
NAM	new approach methodology
NOG	neurite outgrowth
NFA	network formation assay
sc	single-concentration

Tcpl	ToxCast Pipeline

References:

1. Williams AJ; Gaines LGT; Grulke CM; Lowe CN; Sinclair GFB; Samano V; Thillainadarajah I; Meyer B; Patlewicz G; Richard AM, Assembly and Curation of Lists of Per- and Polyfluoroalkyl Substances (PFAS) to Support Environmental Science Research. Frontiers in Environmental Science 2022, 10.
2. OECD, Reconciling Terminology of the Universe of Per- and Polyfluoroalkyl Substances: Recommendations and Practical Guidance. 2021.
3. EPA, U. S. Contaminant Candidate List (CCL) and Regulatory Determination. https://www.epa.gov/ccl/regulatory-determination-4.
4. Convention, S. Stockholm Convention on Persistent Organic Pollutants. http://chm.pops.int/TheConvention/ThePOPs/ChemicalsProposedforListing/tabid/2510/Default.aspx.
5. OECD Portal on Per and Poly Fluorinated Chemicals. https://www.oecd.org/chemicalsafety/portal-perfluorinated-chemicals/countryinformation/european-union.htm (accessed January 12, 2023).
6. Carlson LM; Angrish M; Shirke AV; Radke EG; Schulz B; Kraft A; Judson R; Patlewicz G; Blain R; Lin C; Vetter N; Lemeris C; Hartman P; Hubbard H; Arzuaga X; Davis A; Dishaw LV; Druwe IL; Hollinger H; Jones R; Kaiser JP; Lizarraga L; Noyes PD; Taylor M; Shapiro AJ; Williams AJ; Thayer KA, Systematic Evidence Map for Over One Hundred and Fifty Per- and Polyfluoroalkyl Substances (PFAS). Environ Health Perspect 2022, 130 (5), 56001.
7. Richard AM; Hidle H; Patlewicz G; Williams AJ, Identification of Branched and Linear Forms of PFOA and Potential Precursors: A User-Friendly SMILES Structure-based Approach. Front Environ Sci 2022, 10, 1–865488.
8. Kaboré HA; Vo Duy S; Munoz G; Méité L; Desrosiers M; Liu J; Sory TK; Sauvé S, Worldwide drinking water occurrence and levels of newly-identified perfluoroalkyl and polyfluoroalkyl substances. The Science of the total environment 2018, 616–617, 1089–1100.
9. Ahrens L; Bundschuh M, Fate and effects of poly- and perfluoroalkyl substances in the aquatic environment: a review. Environmental toxicology and chemistry 2014, 33 (9), 1921–9. [PubMed: 24924660]
10. Vestergren R; Cousins IT, Tracking the pathways of human exposure to perfluorocarboxylates. Environ Sci Technol 2009, 43 (15), 5565–75. [PubMed: 19731646]
11. Cao Y; Ng C, Absorption, distribution, and toxicity of per- and polyfluoroalkyl substances (PFAS) in the brain: a review. Environmental science. Processes & impacts 2021, 23 (11), 1623–1640. [PubMed: 34533150]
12. Foguth R; Sepúlveda MS; Cannon J, Per- and Polyfluoroalkyl Substances (PFAS) Neurotoxicity in Sentinel and Non-Traditional Laboratory Model Systems: Potential Utility in Predicting Adverse Outcomes in Human Health. Toxics 2020, 8 (2).
13. Pérez F; Nadal M; Navarro-Ortega A; Fàbrega F; Domingo JL; Barceló D; Farré M, Accumulation of perfluoroalkyl substances in human tissues. Environment international 2013, 59, 354–62. [PubMed: 23892228]
14. Dassuncao C; Pickard H; Pfohl M; Tokranov AK; Li M; Mikkelsen B; Slitt A; Sunderland EM, Phospholipid Levels Predict the Tissue Distribution of Poly- and Perfluoroalkyl Substances in a Marine Mammal. Environmental science & technology letters 2019, 6 (3), 119–125. [PubMed: 33283018]
15. Wang Y; Han W; Wang C; Zhou Y; Shi R; Bonefeld-Jørgensen EC; Yao Q; Yuan T; Gao Y; Zhang J; Tian Y, Efficiency of maternal-fetal transfer of perfluoroalkyl and polyfluoroalkyl substances. Environmental science and pollution research international 2019, 26 (3), 2691–2698. [PubMed: 30484044]
16. Hjermitslev MH; Long M; Wielsøe M; Bonefeld-Jørgensen EC, Persistent organic pollutants in Greenlandic pregnant women and indices of foetal growth: The ACCEPT study. The Science of the total environment 2020, 698, 134118.

17. Blake BE; Fenton SE, Early life exposure to per- and polyfluoroalkyl substances (PFAS) and latent health outcomes: A review including the placenta as a target tissue and possible driver of peri- and postnatal effects. Toxicology 2020, 443, 152565.

18. Liew Z; Goudarzi H; Oulhote Y, Developmental Exposures to Perfluoroalkyl Substances (PFASs): An Update of Associated Health Outcomes. Current environmental health reports 2018, 5 (1), 1–19. [PubMed: 29556975]

19. Rappazzo KM; Coffman E; Hines EP, Exposure to Perfluorinated Alkyl Substances and Health Outcomes in Children: A Systematic Review of the Epidemiologic Literature. International journal of environmental research and public health 2017, 14 (7).

20. Goudarzi H; Nakajima S; Ikeno T; Sasaki S; Kobayashi S; Miyashita C; Ito S; Araki A; Nakazawa H; Kishi R, Prenatal exposure to perfluorinated chemicals and neurodevelopment in early infancy: The Hokkaido Study. The Science of the total environment 2016, 541, 1002–1010. [PubMed: 26473702]

21. Chen MH; Ha EH; Liao HF; Jeng SF; Su YN; Wen TW; Lien GW; Chen CY; Hsieh WS; Chen PC, Perfluorinated compound levels in cord blood and neurodevelopment at 2 years of age. Epidemiology (Cambridge, Mass.) 2013, 24 (6), 800–8. [PubMed: 24036611]

22. Hoffman K; Webster TF; Weisskopf MG; Weinberg J; Vieira VM, Exposure to polyfluoroalkyl chemicals and attention deficit/hyperactivity disorder in U.S. children 12–15 years of age. Environ Health Perspect 2010, 118 (12), 1762–7. [PubMed: 20551004]

23. Ode A; Källén K; Gustafsson P; Rylander L; Jönsson BA; Olofsson P; Ivarsson SA; Lindh CH; Rignell-Hydbom A, Fetal exposure to perfluorinated compounds and attention deficit hyperactivity disorder in childhood. PloS one 2014, 9 (4), e95891.

24. Liew Z; Ritz B; von Ehrenstein OS; Bech BH; Nohr EA; Fei C; Bossi R; Henriksen TB; Bonefeld-Jørgensen EC; Olsen J, Attention deficit/hyperactivity disorder and childhood autism in association with prenatal exposure to perfluoroalkyl substances: a nested case-control study in the Danish National Birth Cohort. Environ Health Perspect 2015, 123 (4), 367–73. [PubMed: 25616253]

25. Gump BB; Wu Q; Dumas AK; Kannan K, Perfluorochemical (PFC) exposure in children: associations with impaired response inhibition. Environ Sci Technol 2011, 45 (19), 8151–9. [PubMed: 21682250]

26. Vuong AM; Webster GM; Yolton K; Calafat AM; Muckle G; Lanphear BP; Chen A, Prenatal exposure to per- and polyfluoroalkyl substances (PFAS) and neurobehavior in US children through 8 years of age: The HOME study. Environmental research 2021, 195, 110825.

27. Oh J; Bennett DH; Calafat AM; Tancredi D; Roa DL; Schmidt RJ; Hertz-Picciotto I; Shin H-M, Prenatal exposure to per- and polyfluoroalkyl substances in association with autism spectrum disorder in the MARBLES study. Environment international 2021, 147, 106328.

28. Oh J; Schmidt RJ; Tancredi D; Calafat AM; Roa DL; Hertz-Picciotto I; Shin H-M, Prenatal exposure to per- and polyfluoroalkyl substances and cognitive development in infancy and toddlerhood. Environmental research 2021, 196, 110939.

29. Fei C; McLaughlin JK; Lipworth L; Olsen J, Prenatal exposure to perfluorooctanoate (PFOA) and perfluorooctanesulfonate (PFOS) and maternally reported developmental milestones in infancy. Environ Health Perspect 2008, 116 (10), 1391–5. [PubMed: 18941583]

30. Forns J; Iszatt N; White RA; Mandal S; Sabaredzovic A; Lamoree M; Thomsen C; Haug LS; Stigum H; Eggesbø M, Perfluoroalkyl substances measured in breast milk and child neuropsychological development in a Norwegian birth cohort study. Environment international 2015, 83, 176–82. [PubMed: 26159671]

31. Strøm M; Hansen S; Olsen SF; Haug LS; Rantakokko P; Kiviranta H; Halldorsson TI, Persistent organic pollutants measured in maternal serum and offspring neurodevelopmental outcomes--a prospective study with long-term follow-up. Environment international 2014, 68, 41–8. [PubMed: 24704638]

32. Johansson N; Fredriksson A; Eriksson P, Neonatal exposure to perfluorooctane sulfonate (PFOS) and perfluorooctanoic acid (PFOA) causes neurobehavioural defects in adult mice. Neurotoxicology 2008, 29 (1), 160–9. [PubMed: 18063051]

33. Hallgren S; Fredriksson A; Viberg H, More signs of neurotoxicity of surfactants and flame retardants - Neonatal PFOS and PBDE 99 cause transcriptional alterations in cholinergic genes in the mouse CNS. Environ Toxicol Pharmacol 2015, 40 (2), 409–16. [PubMed: 26254212]
34. Sobolewski M; Conrad K; Allen JL; Weston H; Martin K; Lawrence BP; Cory-Slechta DA, Sex-specific enhanced behavioral toxicity induced by maternal exposure to a mixture of low dose endocrine-disrupting chemicals. Neurotoxicology 2014, 45, 121–30. [PubMed: 25454719]
35. Fuentes S; Vicens P; Colomina MT; Domingo JL, Behavioral effects in adult mice exposed to perfluorooctane sulfonate (PFOS). Toxicology 2007, 242 (1–3), 123–9. [PubMed: 17950980]
36. Sachana M; Shafer TJ; Terron A, Toward a Better Testing Paradigm for Developmental Neurotoxicity: OECD Efforts and Regulatory Considerations. Biology (Basel) 2021, 10 (2).
37. Carstens KE; Carpenter AF; Martin MM; Harrill JA; Shafer TJ; Paul Friedman K, Integrating Data From In Vitro New Approach Methodologies for Developmental Neurotoxicity. Toxicol Sci 2022, 187 (1), 62–79. [PubMed: 35172012]
38. Bal-Price A; Hogberg HT; Crofton KM; Daneshian M; FitzGerald RE; Fritsche E; Heinonen T; Hougaard Bennekou S; Klima S; Piersma AH; Sachana M; Shafer TJ; Terron A; Monnet-Tschudi F; Viviani B; Waldmann T; Westerink RHS; Wilks MF; Witters H; Zurich MG; Leist M, Recommendation on test readiness criteria for new approach methods in toxicology: Exemplified for developmental neurotoxicity. Altex 2018, 35 (3), 306–352. [PubMed: 29485663]
39. Brown JP; Hall D; Frank CL; Wallace K; Mundy WR; Shafer TJ, Editor's Highlight: Evaluation of a Microelectrode Array-Based Assay for Neural Network Ontogeny Using Training Set Chemicals. Toxicol Sci 2016, 154 (1), 126–139. [PubMed: 27492221]
40. Frank CL; Brown JP; Wallace K; Mundy WR; Shafer TJ, From the Cover: Developmental Neurotoxicants Disrupt Activity in Cortical Networks on Microelectrode Arrays: Results of Screening 86 Compounds During Neural Network Formation. Toxicol Sci 2017, 160 (1), 121–135. [PubMed: 28973552]
41. Shafer TJ; Brown JP; Lynch B; Davila-Montero S; Wallace K; Friedman KP, Evaluation of Chemical Effects on Network Formation in Cortical Neurons Grown on Microelectrode Arrays. Toxicol Sci 2019, 169 (2), 436–455. [PubMed: 30816951]
42. Druwe I; Freudenrich TM; Wallace K; Shafer TJ; Mundy WR, Sensitivity of neuroprogenitor cells to chemical-induced apoptosis using a multiplexed assay suitable for high-throughput screening. Toxicology 2015, 333, 14–24. [PubMed: 25841707]
43. Harrill JA; Freudenrich TM; Machacek DW; Stice SL; Mundy WR, Quantitative assessment of neurite outgrowth in human embryonic stem cell-derived hN2 cells using automated high-content image analysis. Neurotoxicology 2010, 31 (3), 277–90. [PubMed: 20188755]
44. Filer DL; Kothiya P; Setzer RW; Judson RS; Martin MT, tcpl: the ToxCast pipeline for high-throughput screening data. Bioinformatics 2017, 33 (4), 618–620. [PubMed: 27797781]
45. Patlewicz G; Richard AM; Williams AJ; Grulke CM; Sams R; Lambert J; Noyes PD; DeVito MJ; Hines RN; Strynar M; Guiseppi-Elie A; Thomas RS, A Chemical Category-Based Prioritization Approach for Selecting 75 Per- and Polyfluoroalkyl Substances (PFAS) for Tiered Toxicity and Toxicokinetic Testing. Environ Health Perspect 2019, 127 (1), 14501. [PubMed: 30632786]
46. Liberatore HK; Jackson SR; Strynar MJ; McCord JP, Solvent Suitability for HFPO-DA ("GenX" Parent Acid) in Toxicological Studies. Environmental science & technology letters 2020, 7 (7), 477–481. [PubMed: 32944590]
47. Mundy WR; Padilla S; Breier JM; Crofton KM; Gilbert ME; Herr DW; Jensen KF; Radio NM; Raffaele KC; Schumacher K; Shafer TJ; Cowden J, Expanding the test set: Chemicals with potential to disrupt mammalian brain development. Neurotoxicol Teratol 2015, 52 (Pt A), 25–35. [PubMed: 26476195]
48. Smeltz MG; Clifton MS; Henderson WM; McMillan L; Wetmore BA, Targeted Per- and Polyfluoroalkyl substances (PFAS) assessments for high throughput screening: Analytical and testing considerations to inform a PFAS stock quality evaluation framework. Toxicol Appl Pharmacol 2022, 459, 116355.
49. Bader BM; Steder A; Klein AB; Frølund B; Schroeder OHU; Jensen AA, Functional characterization of GABAA receptor-mediated modulation of cortical neuron network activity in microelectrode array recordings. PloS one 2017, 12 (10), e0186147.

50. Paul Friedman K; Gagne M; Loo LH; Karamertzanis P; Netzeva T; Sobanski T; Franzosa JA; Richard AM; Lougee RR; Gissi A; Lee JJ; Angrish M; Dorne JL; Foster S; Raffaele K; Bahadori T; Gwinn MR; Lambert J; Whelan M; Rasenberg M; Barton-Maclaren T; Thomas RS, Utility of In Vitro Bioactivity as a Lower Bound Estimate of In Vivo Adverse Effect Levels and in Risk-Based Prioritization. Toxicol Sci 2020, 173 (1), 202–225. [PubMed: 31532525]
51. Ward JM, Hierarchical Grouping to Optimize an Objective Function. Journal of the American Statistical Association 1963, 58, 236–244.
52. Warnes GR; Bolker B; Bonebakker L; Gentleman R; Liaw WHA; Lumley T, Package 'gplots': various r programming tools for plotting data. R package version 3.0. 1. 2016.
53. Houck KA; Dix DJ; Judson RS; Kavlock RJ; Yang J; Berg EL, Profiling bioactivity of the ToxCast chemical library using BioMAP primary human cell systems. J Biomol Screen 2009, 14 (9), 1054–66. [PubMed: 19773588]
54. Houck KA PFK, Feshuk M, Patlewicz G, Smeltz M, Clifton MS, Wetmore BA, Velichko S, Berenyi A, Berg E. (In Review) Evaluation of 147 Perfluoroalkyl Substances for Immunotoxic and other (Patho)physiological Activities through Phenotypic Screening of Human Primary Cells. 2022.
55. Houck KA; Patlewicz G; Richard AM; Williams AJ; Shobair MA; Smeltz M; Clifton MS; Wetmore B; Medvedev A; Makarov S, Bioactivity profiling of per- and polyfluoroalkyl substances (PFAS) identifies potential toxicity pathways related to molecular structure. Toxicology 2021, 457, 152789.
56. Medvedev A; Moeser M; Medvedeva L; Martsen E; Granick A; Raines L; Zeng M; Makarov S Jr.; Houck KA; Makarov SS, Evaluating biological activity of compounds by transcription factor activity profiling. Science advances 2018, 4 (9), eaar4666.
57. OECD/UNEP, Reconciling Terminology of the Universe of Per- and Polyfluoroalkyl Substances: Recommendations and Practical Guidance. Organisation for Economic Co-operation and Development; Environmental Directorate Chemicals and Biotechnology Committee 2021.
58. Su A; Rajan K, A database framework for rapid screening of structure-function relationships in PFAS chemistry. Scientific data 2021, 8 (1), 14. [PubMed: 33462239]
59. Mansouri K; Grulke CM; Judson RS; Williams AJ, OPERA models for predicting physicochemical properties and environmental fate endpoints. Journal of cheminformatics 2018, 10 (1), 10. [PubMed: 29520515]
60. Williams AJ; Lambert JC; Thayer K; Dorne JCM, Sourcing data on chemical properties and hazard data from the US-EPA CompTox Chemicals Dashboard: A practical guide for human risk assessment. Environment international 2021, 154, 106566.
61. Yang C; Tarkhov A; Marusczyk J; Bienfait B; Gasteiger J; Kleinoeder T; Magdziarz T; Sacher O; Schwab CH; Schwoebel J; Terfloth L; Arvidson K; Richard A; Worth A; Rathman J, New publicly available chemical query language, CSRML, to support chemotype representations for application to data mining and modeling. Journal of chemical information and modeling 2015, 55 (3), 510–28. [PubMed: 25647539]
62. Patlewicz G RA, Williams AJ, Judson RS, Thomas RS, Towards reproducible structure-based chemical categories for PFAS to inform and evaluate toxicity and toxicokinetic testing. (In preparation).
63. Wang J; Richard AM; Murr AS; Buckalew AR; Lougee RR; Shobair M; Hallinger DR; Laws SC; Stoker TE, Expanded high-throughput screening and chemotype-enrichment analysis of the phase II: e1k ToxCast library for human sodium-iodide symporter (NIS) inhibition. Arch Toxicol 2021, 95 (5), 1723–1737. [PubMed: 33656581]
64. EPA, U. S. Exploring ToxCast Data: Downloadable Data. https://www.epa.gov/chemical-research/exploring-toxcast-data-downloadable-data.
65. Houck KA; Friedman KP; Feshuk M; Patlewicz G; Smeltz M; Clifton MS; Wetmore BA; Velichko S; Berenyi A; Berg EL, Evaluation of 147 perfluoroalkyl substances for immunotoxic and other (patho)physiological activities through phenotypic screening of human primary cells. Altex 2022.
66. Harrill JA; Freudenrich T; Wallace K; Ball K; Shafer TJ; Mundy WR, Testing for developmental neurotoxicity using a battery of in vitro assays for key cellular events in neurodevelopment. Toxicol Appl Pharmacol 2018, 354, 24–39. [PubMed: 29626487]

67. Rice D; Barone S Jr., Critical periods of vulnerability for the developing nervous system: evidence from humans and animal models. Environ Health Perspect 2000, 108 Suppl 3 (Suppl 3), 511–33. [PubMed: 10852851]
68. Onishchenko N; Fischer C; Wan Ibrahim WN; Negri S; Spulber S; Cottica D; Ceccatelli S, Prenatal exposure to PFOS or PFOA alters motor function in mice in a sex-related manner. Neurotoxicity research 2011, 19 (3), 452–61. [PubMed: 20512442]
69. Spulber S; Kilian P; Wan Ibrahim WN; Onishchenko N; Ulhaq M; Norrgren L; Negri S; Di Tuccio M; Ceccatelli S, PFOS induces behavioral alterations, including spontaneous hyperactivity that is corrected by dexamfetamine in zebrafish larvae. PloS one 2014, 9 (4), e94227.
70. Gaballah S; Swank A; Sobus JR; Howey XM; Schmid J; Catron T; McCord J; Hines E; Strynar M; Tal T, Evaluation of Developmental Toxicity, Developmental Neurotoxicity, and Tissue Dose in Zebrafish Exposed to GenX and Other PFAS. Environ Health Perspect 2020, 128 (4), 47005.
71. CDC, Fourth national report on human exposure to environmental chemicals: updated tables, January 2019, Volume one. 2019.
72. Liao C; Wang T; Cui L; Zhou Q; Duan S; Jiang G, Changes in synaptic transmission, calcium current, and neurite growth by perfluorinated compounds are dependent on the chain length and functional group. Environ Sci Technol 2009, 43 (6), 2099–104. [PubMed: 19368220]
73. Menger F; Pohl J; Ahrens L; Carlsson G; Örn S, Behavioural effects and bioconcentration of per- and polyfluoroalkyl substances (PFASs) in zebrafish (Danio rerio) embryos. Chemosphere 2020, 245, 125573.
74. Ulhaq M; Carlsson G; Örn S; Norrgren L, Comparison of developmental toxicity of seven perfluoroalkyl acids to zebrafish embryos. Environ Toxicol Pharmacol 2013, 36 (2), 423–426. [PubMed: 23770452]
75. Ammazzalorso A; De Filippis B; Giampietro L; Amoroso R, N-acylsulfonamides: Synthetic routes and biological potential in medicinal chemistry. Chemical biology & drug design 2017, 90 (6), 1094–1105. [PubMed: 28632928]
76. Mahapatra CT; Damayanti NP; Guffey SC; Serafin JS; Irudayaraj J; Sepúlveda MS, Comparative in vitro toxicity assessment of perfluorinated carboxylic acids. Journal of applied toxicology : JAT 2017, 37 (6), 699–708. [PubMed: 27917506]
77. Goss KU, The pKa values of PFOA and other highly fluorinated carboxylic acids. Environ Sci Technol 2008, 42 (2), 456–8. [PubMed: 18284146]
78. Shah P; Westwell AD, The role of fluorine in medicinal chemistry. Journal of enzyme inhibition and medicinal chemistry 2007, 22 (5), 527–40. [PubMed: 18035820]
79. Gomis MI; Vestergren R; Borg D; Cousins IT, Comparing the toxic potency in vivo of long-chain perfluoroalkyl acids and fluorinated alternatives. Environment international 2018, 113, 1–9. [PubMed: 29421396]
80. Droge STJ, Membrane-Water Partition Coefficients to Aid Risk Assessment of Perfluoroalkyl Anions and Alkyl Sulfates. Environ Sci Technol 2019, 53 (2), 760–770. [PubMed: 30572703]
81. Beesoon S; Martin JW, Isomer-Specific Binding Affinity of Perfluorooctanesulfonate (PFOS) and Perfluorooctanoate (PFOA) to Serum Proteins. Environ Sci Technol 2015, 49 (9), 5722–31. [PubMed: 25826685]
82. Weaver YM; Ehresman DJ; Butenhoff JL; Hagenbuch B, Roles of rat renal organic anion transporters in transporting perfluorinated carboxylates with different chain lengths. Toxicol Sci 2010, 113 (2), 305–14. [PubMed: 19915082]
83. Ferguson CS; Tyndale RF, Cytochrome P450 enzymes in the brain: emerging evidence of biological significance. Trends in pharmacological sciences 2011, 32 (12), 708–14. [PubMed: 21975165]
84. Si J; Li J; Zhang F; Li G; Xin Q; Dai B, Effects of perinatal exposure to low doses of tributyltin chloride on pregnancy outcome and postnatal development in mouse offspring. Environmental toxicology 2012, 27 (10), 605–12. [PubMed: 22972585]
85. Newland MC; Rasmussen EB, Aging unmasks adverse effects of gestational exposure to methylmercury in rats. Neurotoxicol Teratol 2000, 22 (6), 819–28. [PubMed: 11120387]

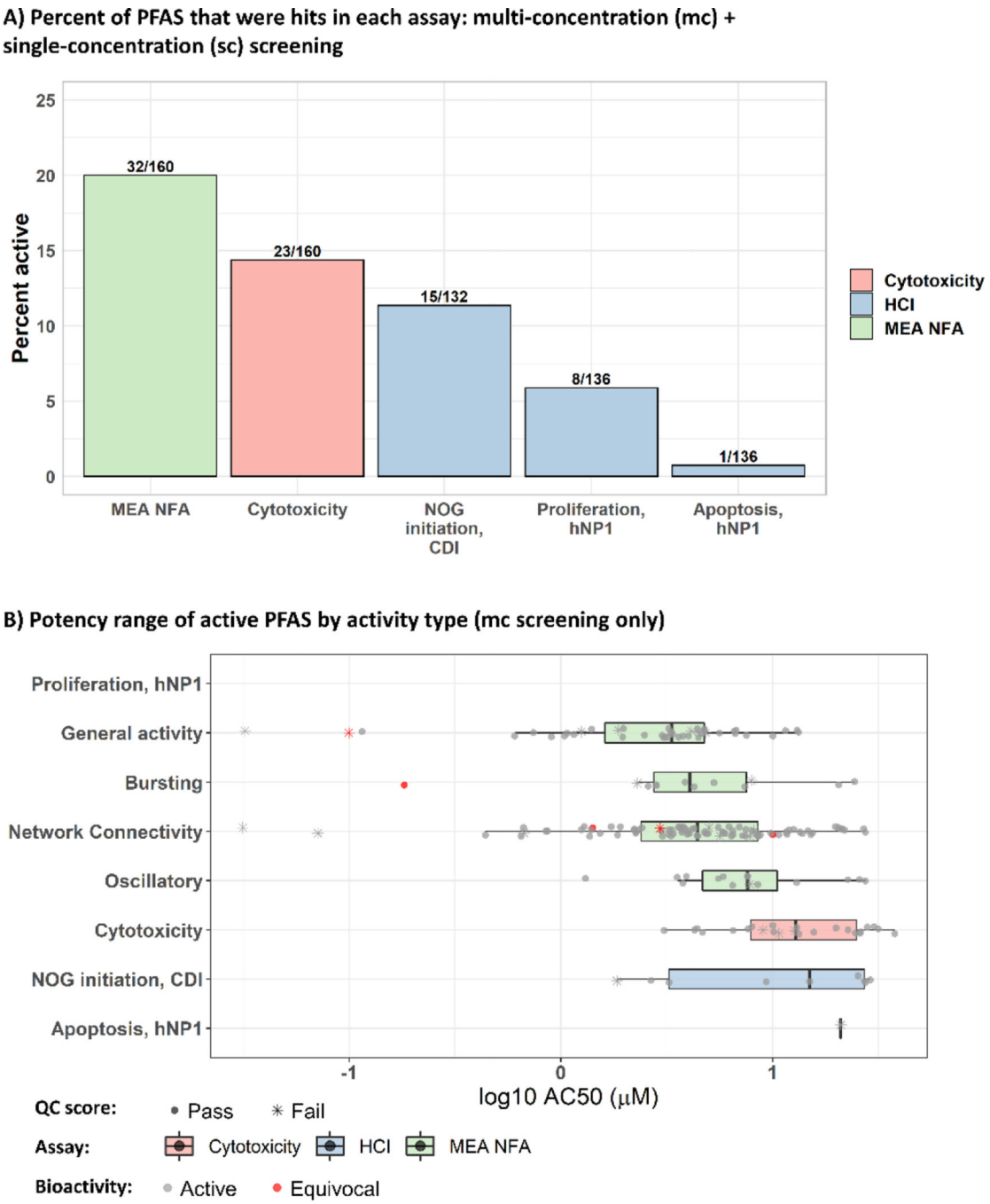

Figure 1:

DNT NAMs activity by assay and activity types

A: The percentage of active PFAS in mc and sc screening by neurodevelopemntal process (MEA NFA, NOG, apoptosis, and proliferation). The fraction represents the total number of active PFAS/ the total number of PFAS screened in the assay. B: The potency range of bioactivity by activity type, with median and interquartile range shown in a boxplot. Superimposed data points (represented by the boxplot) denote the concentration at 50% maximal activity for each positive hit-call in the mc screening (log10 AC50 (μM)).

The legend indicates the assay technology for each group. Cytotoxicity includes all measurements of cytotoxicy from each assay in the battery. MEA NFA: microelectrode array network formation assay, HCI: high content imaging, NOG: neurite outgrowth assay.The shape of the data points corresponds to the QC results of “Pass” (dot) or “Fail” (asterisk) and the color corresponds to the bioactivity determination of “Active” (gray) or “Equivocal” (red).

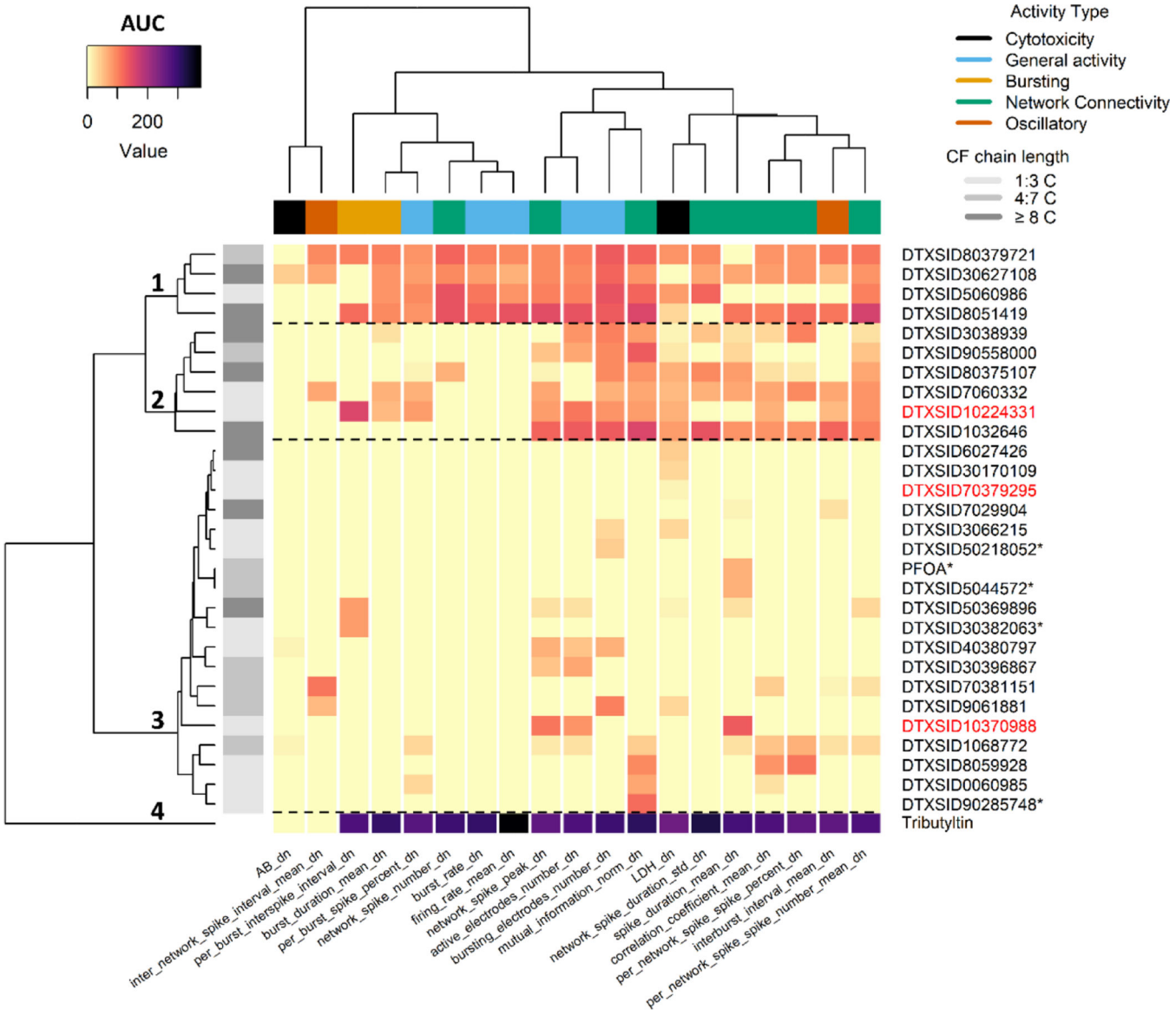

Figure 2:

Heatmap of PFAS efficacy and/or potency in the MEA NFA

Rows of the heatmap indicate chemical activity in each activity type. Column color legend indicates the efficacy and potency as measured by an area under the curve (AUC) metric. Yellow indicates inactivity (AUC of zero), whereas increasing pink to black colors indicates increasing AUC values (higher efficacy and/or potency). Tributyltin is included as a compound with demonstrated DNT NAMs activity from historical data. Color of row text label (right) indicates whether the PFAS passed QC (black) or failed QC (red). An asterisk following the row text label indicates that the PFAS bioactivity was equivocal. Row color legend (left) indicates the number of C atoms in each chemical binned into three groups.

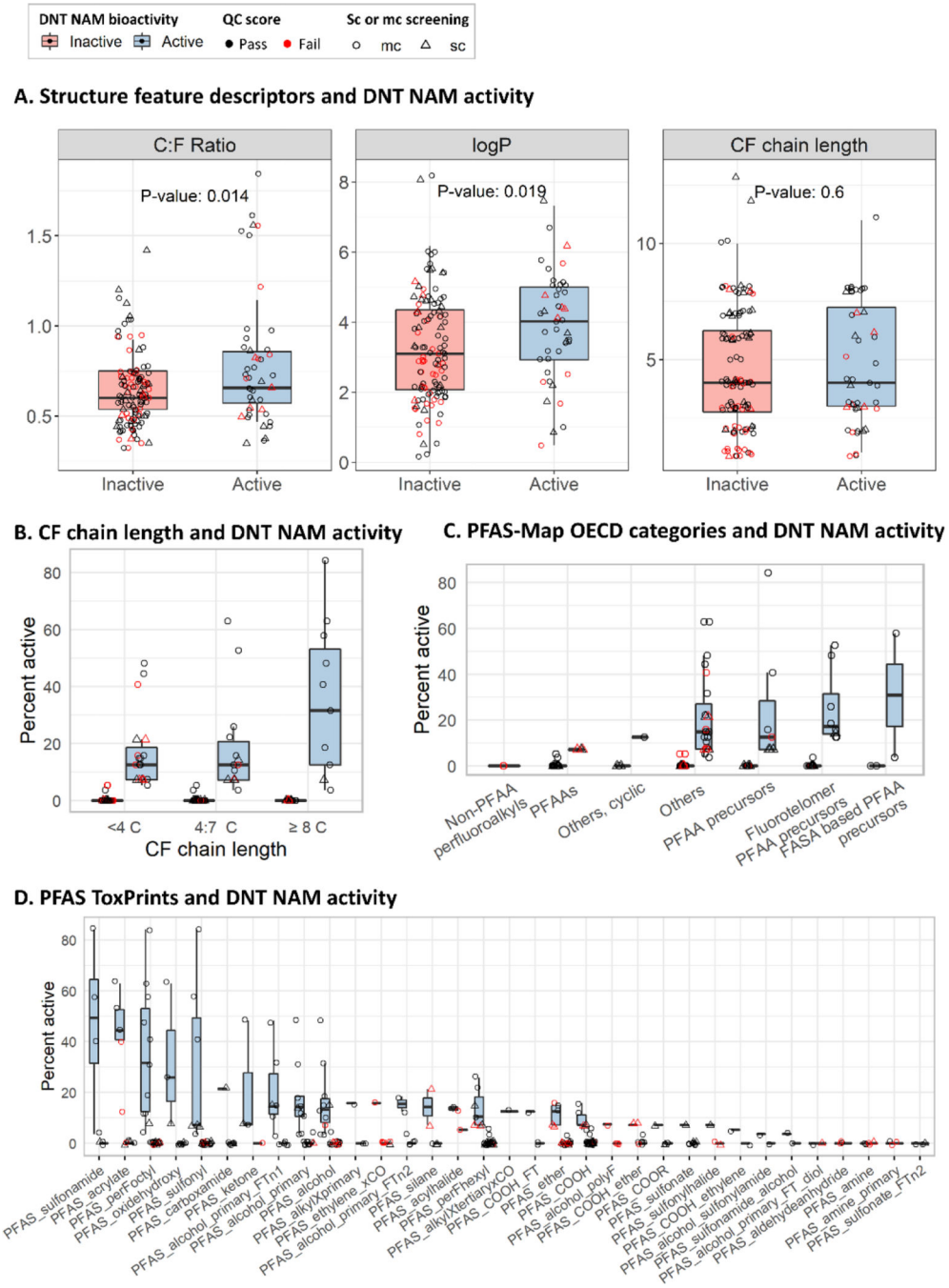

Figure 3:

Chemical and structure feature descriptors and DNT NAMs activity

Box plots showing trends in PFAS sc and mc activity in the DNT NAMs battery and chemical and structure feature descriptors. An ‘active’ (blue boxplot fill) was defined as a chemical that demonstrated a positive response in at least one endpoint in either sc or mc screening (triangle or circle shapes, respectively). An ‘inactive’ (red boxplot fill) includes chemicals demonstrating no activity or equivocal activity. Box plots indicate the median, lower 25th percentile, and upper 75th percentile. Data point color indicates QC testing

results; pass (black), fail (red). A: The C:F ratio, logP, and CF chain length were compared between inactive and active PFAS with a Student's T-test for significance ($p < 0.05$). The percent activity of each chemical in the battery (number of positive hit-calls/ number of tested endpoints *100) were plotted against B: the CF chain length, binned into three groups (<4 C, 4:7 C, and ≥8 C), C: the PFAS-map OECD structure categories, and D: PFAS ToxPrints.

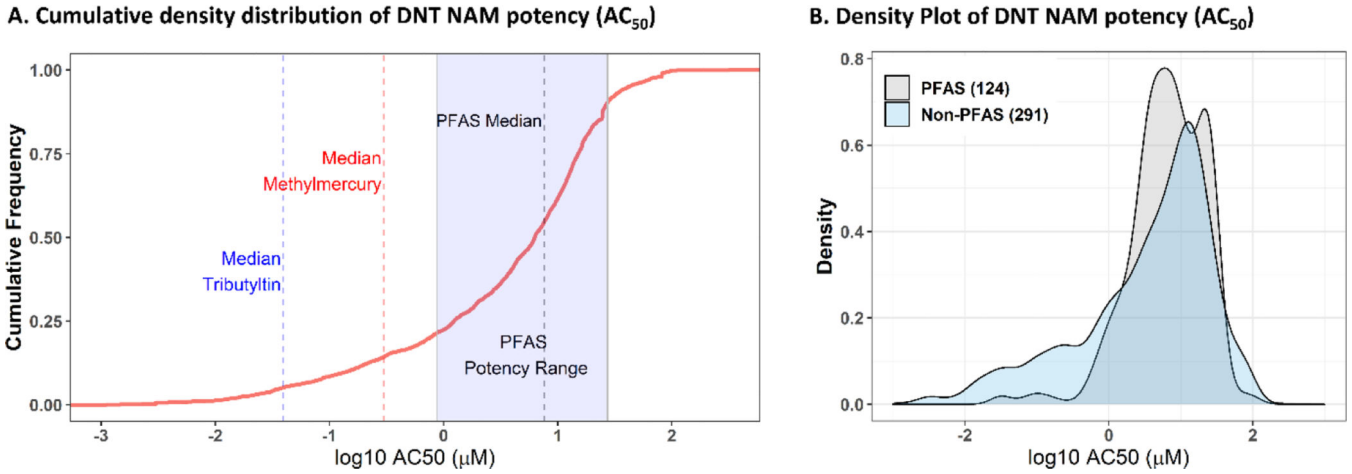

Figure 4:

PFAS bioactivity compared to all available chemicals tested in the DNT NAMs battery. A: A cumulative density distribution plot of potencies (AC_{50}) from all available DNT NAMs data (415 chemicals, red line) compared to the distribution of the median PFAS potency (blue rectangle with a minimum x-axis value of the 5^{th} %-ile PFAS AC_{50} and a maximum x-axis value of the 95^{th} %-ile PFAS AC_{50}) compared to the average potency of two known neurodevelopmental toxicants, methylmercury (blue dotted line) and tributyltin (red dotted line). B: A density plot comparing active PFAS potencies (AC_{50}) (gray) to all other active non-PFAS chemicals (a total of 291 chemicals) in the DNT NAMs battery (blue). The x-axis units are in log10-μM.

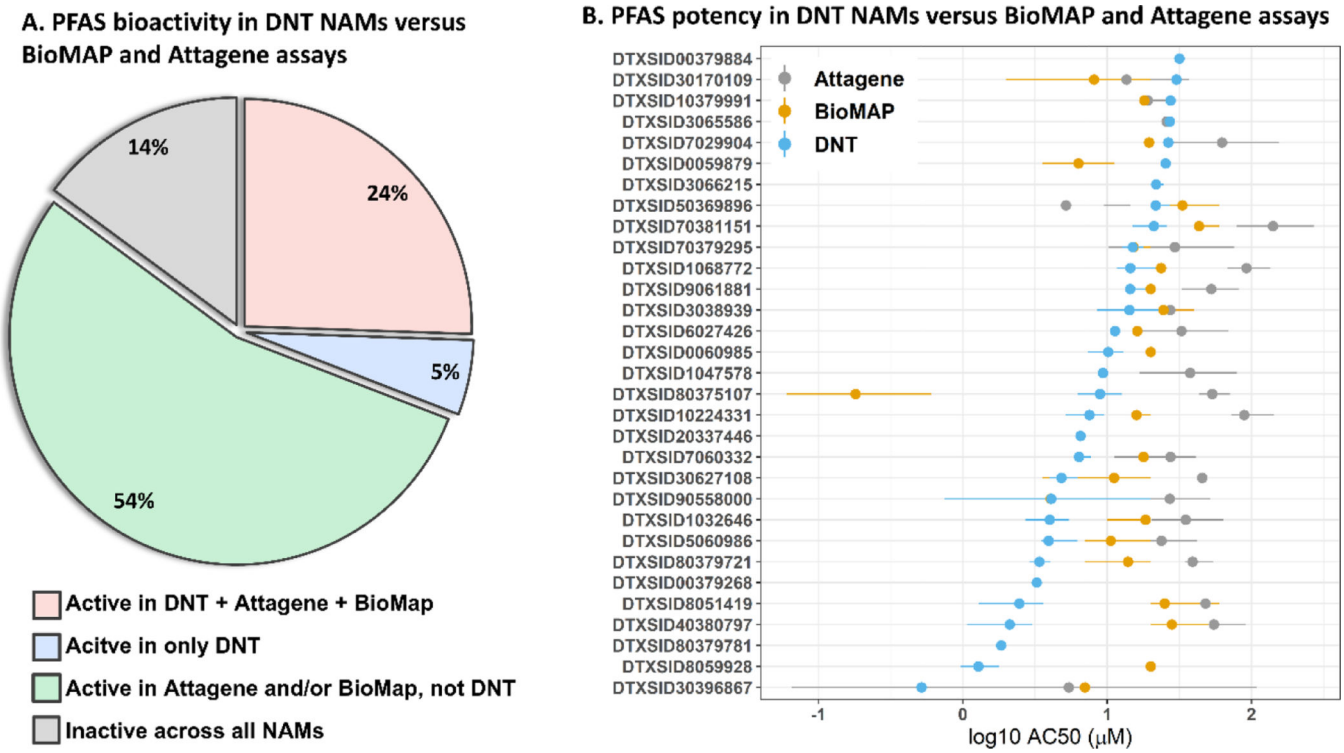

Figure 5.

PFAS potency in the DNT NAMs as compared to the potency in the BioMAP and Attagene assays.

A: The pie chart shows the percent of PFAS that were active in only the DNT NAMs compared to BioMAP and Attagene assays. B: The data indicate the mean AC_{50} values for PFAS that were active across all three assays (Attagene, BioMAP, or DNT NAMs). The lines indicate the lower (0.25) and upper (0.75) quantile bounds.

Table 1.

List of DNT NAMs endpoints measured in multiple-concentration (mc) or single-concentration (sc) screening in the MEA NFA or HCI assay technologies.

	Endpoint	mc	sc	Activity Type	Technology	Cell type
HCI						
1	CCTE_Mundy_HCI_CDI_NOG_BPCount_loss	x	x	NOG	HCI	Human
2	CCTE_Mundy_HCI_CDI_NOG_NeuriteCount_loss	x	x	NOG	HCI	Human
3	CCTE_Mundy_HCI_CDI_NOG_NeuriteLength_loss	x	x	NOG	HCI	Human
4	CCTE_Mundy_HCI_CDI_NOG_NeuronCount_loss	x	x	Cytotoxicity (NOG)	HCI	Human
5	CCTE_Mundy_HCI_hNP1_Casp3_7_gain	x	x	Apoptosis	HCI	Human
6	CCTE_Mundy_HCI_hNP1_CellTiter_loss	x	x	Cytotoxicity (Apop)	HCI	Human
7	CCTE_Mundy_HCI_hNP1_Pro_ObjectCount_loss	x	x	Cytotoxicity (Prolif)	HCI	Human
8	CCTE_Mundy_HCI_hNP1_Pro_ResponderAvgInten_loss	x	x	Proliferation	HCI	Human
MEA NFA						
1	CCTE_Shafer_MEA_dev_active_electrodes_number_dn	x		General activity	MEA NFA	Rat
2	CCTE_Shafer_MEA_dev_burst_rate_dn	x		General activity	MEA NFA	Rat
3	CCTE_Shafer_MEA_dev_bursting_electrodes_number_dn	x	x	General activity	MEA NFA	Rat
4	CCTE_Shafer_MEA_dev_firing_rate_mean_dn	x		General activity	MEA NFA	Rat
5	CCTE_Shafer_MEA_dev_per_burst_spike_percent_dn	x		General activity	MEA NFA	Rat
6	CCTE_Shafer_MEA_dev_burst_duration_mean_dn	x		Bursting	MEA NFA	Rat
7	CCTE_Shafer_MEA_dev_per_burst_interspike_interval_dn	x		Bursting	MEA NFA	Rat
8	CCTE_Shafer_MEA_dev_correlation_coefficient_mean_dn	x		Network Connectivity	MEA NFA	Rat
9	CCTE_Shafer_MEA_dev_mutual_information_norm_dn	x	x	Network Connectivity	MEA NFA	Rat
10	CCTE_Shafer_MEA_dev_network_spike_duration_std_dn	x		Network Connectivity	MEA NFA	Rat
11	CCTE_Shafer_MEA_dev_network_spike_number_dn	x		Network Connectivity	MEA NFA	Rat
12	CCTE_Shafer_MEA_dev_network_spike_peak_dn	x	x	Network Connectivity	MEA NFA	Rat
13	CCTE_Shafer_MEA_dev_per_network_spike_spike_number_mean_dn	x		Network Connectivity	MEA NFA	Rat
14	CCTE_Shafer_MEA_dev_per_network_spike_spike_percent_dn	x		Network Connectivity	MEA NFA	Rat
15	CCTE_Shafer_MEA_dev_spike_duration_mean_dn	x		Network Connectivity	MEA NFA	Rat
16	CCTE_Shafer_MEA_dev_inter_network_spike_interval_mean_dn	x	x	Oscillatory	MEA NFA	Rat
17	CCTE_Shafer_MEA_dev_interburst_interval_mean_dn	x		Oscillatory	MEA NFA	Rat
18	CCTE_Shafer_MEA_dev_LDH_dn	x	x	Cytotoxicity	MEA NFA	Rat
19	CCTE_Shafer_MEA_dev_AB_dn	x	x	Cytotoxicity	MEA NFA	Rat

Table 2:

DNT NAMs bioactivity of seven selected PFAS

The total number of positive responses (hit sum) out of the total number of endpoints tested (N tested endpoints) is shown for multi-concentration (mc) or single-concentration (sc). PFAS were given a QC grade of either pass (P) or fail (F). QC flags include ‘Z’ (MW Confirmed, No Purity Info), ‘Fns’ (caution, no sample detected, biological activity unreliable), ‘Fde’ (caution, degradation of analyte evident, in some instances due to DMSO), ‘P’ (pseudo-parent monitored or adduct monitored; no direct confirmation that parent analyte is present), and ‘I’ (Isomers; two or more isomers detected).

PFAS	DTXSID	QC Pass/ Fail	QC.flags	Mc hit sum	Mc N tested endpoints	SC hit sum	Sc N tested endpoints	Bioactivity
PFOA	DTXSID8031865	P	Z	1	19			Equivocal
GenX	DTXSID70880215	F	Fns, Fde, P	0	27			Inactive
PFOS	DTXSID3031864	P	Z, I	0	27			Inactive
PFHxA	DTXSID3031862	P	Z	0	19			Inactive
PFBS	DTXSID5030030	P	Z	0	19			Inactive
PFHpS	DTXSID8059920	P	Z			1	14	Equivocal
PFHxS	DTXSID7040150	P	Z, I			0	14	Inactive

Table 3:

PFAS with the highest DNT NAMs bioactivity

PFAS with the highest bioactivity were defined as PFAS that demonstrated more than 30% activity in the tested endpoints in the DNT NAMs battery. Percent activity was computed as number of positive responses/ total number of screened endpoints * 100. QC results (pass (P) or fail (F)) and QC flags include 'Z' (MW Confirmed, No Purity Info), 'I' (Isomers; two or more isomers detected),), 'P' (pseudo-parent monitored or adduct monitored, 'M' (defined Mixture; 2 or more components), and 'Fde' (caution, degradation of analyte evident, in some instances due to DMSO; no direct confirmation that parent analyte is present) are included. 'Txp_PFAS_34cats' indicates the PFAS ToxPrint categories contained in the PFAS chemical structure.

PFAS	DTXSID	Percent active	QC result	QC flags	CF chain length	C:F Ratio	Mean AC_{50} (log10-μM)	Mean AC_{50} (μM)	TxP_PFAS_34cat
N-[(Perfluorooctylsulfonamido)propyl]-N,N,N-trimethylammonium iodide	DTXSID8051419	84.21	P	Z, I, P	8	0.82	0.33	2.13	PFAS_sulfonyl; PFAS_sulfonamide; PFAS_perFoctyl
1H,1H,6H,6H-Perfluorohexane-1,6-diol diacrylate	DTXSID80379721	62.96	P	Z	4	1.50	0.51	3.20	PFAS_acrylate
((Perfluorooctyl)ethyl)phos phonic acid	DTXSID30627108	62.96	P	E	8	0.59	0.67	4.66	PFAS_oxidehydroxy; PFAS_perFoctyl
N-Ethylperfluorooctanesulfon amide	DTXSID1032646	57.89	P	I, M	8	0.59	0.44	2.78	PFAS_sulfonyl; PFAS_sulfonamide; PFAS_perFoctyl
2-(Perfluorobutyl)ethyl acrylate	DTXSID1068772	52.63	P	Z	4	1.00	1.14	13.80	PFAS_acrylate
11:1 Fluorotelomer alcohol	DTXSID80375107	48.15	P	Z	11	0.52	0.77	5.87	PFAS_alcohol; PFAS_alcohol_primary; PFAS_alcohol_primary_FTn1; PFAS_perFoctyl
(Perfluorobutyryl)-2-thenoylmethane	DTXSID7060332	48.15	P	Z	3	1.43	0.78	5.99	PFAS_ketone
1H,1H,5H,5H-Perfluoro-1,5-pentanediol diacrylate	DTXSID5060986	44.44	P	Z	3	1.83	0.45	2.84	PFAS_acrylate
2,2,3,3-Tetrafluoropropyl acrylate	DTXSID10224331	40.74	F	Fde	2	1.50	0.76	5.70	PFAS_acrylate
Perfluorooctanesulfonamide	DTXSID3038939	40.74	P	Z, I	8	0.47	1.08	12.14	PFAS_sulfonyl; PFAS_sulfonamide; PFAS_perFoctyl
1H,1H,10H,10H-Perfluorodecane-1,10-diol	DTXSID50369896	31.58	P	Z	8	0.63	1.26	18.25	PFAS_alcohol; PFAS_alcohol_primary; PFAS_alcohol_primary_FTn1; PFAS_perFoctyl